1-1-2015

Mesoarchaean collision of Kapisilik terrane 3070Ma juvenile arc rocks and >3600Ma Isukasia terrane continental crust (Greenland)

Allen Phillip Nutman
University of Wollongong, anutman@uow.edu.au

Vickie C. Bennett
Australian National University, vickie.bennett@anu.edu.au

Clark R. L Friend
Gendale, UK

Keewook Yi
Korea Institute of Geoscience and Mineral Resources

Seung Ryeol Lee
Korea Institute of Geoscience and Mineral Resources

Mesoarchaean collision of Kapisilik terrane 3070Ma juvenile arc rocks and >3600Ma Isukasia terrane continental crust (Greenland)

Abstract

The Mesoarchaean Kapisilik and Eoarchaean Isukasia terranes in the Nuuk region of southern West Greenland were tectonically juxtaposed in the Archaean. The north of the Isukasia terrane is distal from the Kapisilik terrane and has only rare growth of ~2690Ma metamorphic zircon and no 2980-2950Ma metamorphic zircon. The southern part of the Isukasia terrane lies between two ~2690Ma shear zones, and has locally preserved high pressure granulite facies assemblages and widespread growth of 2980-2950Ma metamorphic zircon and also sporadic growth of ~2690Ma metamorphic zircon. Within this southern part of the Isukasia terrane there is a folded klippe of mylonitised Mesoarchaean detrital meta-sedimentary rocks (carrying >3600 and ~3070Ma detrital zircons), mafic and ultramafic rocks, with ~2970Ma metamorphic zircon overgrowths. South of the Isukasia terrane is the Kapisilik terrane, containing ~3070Ma arc-related volcanic rocks, gabbro-anorthosites and meta-tonalites, intruded by 2970-2960Ma granites. Zircons of an Ivisârtoq supracrustal belt ~3075Ma intermediate volcanic rock have initial e{open}Hf values of +2 to +5 thus are juvenile crustal additions. ~3070Ma tonalites along the northern edge of the Kapisilik terrane have whole rock positive initial e{open}Nd values and thus are also juvenile crustal additions. In contrast, igneous zircons in 2960Ma granites intruded into juvenile ~3075Ma supracrustal rocks of the Kapisilik terrane have initial e{open}Hf values of -5 to -10, and must have involved the partial melting of >3600Ma Isukasia terrane rocks.The integrated structural and zircon U-Th-Pb-Hf isotopic data show that at 2980-2950. Ma the Kapisilik terrane juvenile arc components collided with, and over-rid, the Isukasia terrane. The southern edge of the Isukasia terrane came to lie in the deep crust under the Ivisârtoq supracrustal belt and melted at 2970-2960. Ma to produce granites. These granites derived from ancient crust rose into the upper crust, where they intruded the overlying allochthonous juvenile ~3075. Ma Ivisârtoq supracrustal belt arc assemblages. The southern edge of the Isukasia terrane is interpreted as an interior nappe of Eoarchaean basement rocks interfolded with a klippe of Mesoarchaean metasedimentary and mafic/ultramafic rocks, both of which are affected by 2980-2950. Ma metamorphism. The mixed Eoarchaean-Mesoarchaean detrital provenance suggests that the klippe could be dismembered components of an accretionary prism or forearc crust. The northern part of the Isukasia terrane is interpreted as foreland, free of 2980-2950. Ma high-grade metamorphic overprint. This shows that the Isukasia terrane is not a coherent block, but contains ancient rocks that are parautochthonous or allochthonous to each other, with contrasting later metamorphic history.At ~2690. Ma the crustal architecture arisen from Mesoarchaean collision between an older continental block and an island arc was reworked along intra-crustal shear zones, coeval with amphibolite facies metamorphism. This reworking followed on from major terrane assembly at 2710-2700. Ma in the southern part of the Nuuk region, when the Eoarchaean Færingehavn terrane was juxtaposed with 2840-2825. Ma arc rocks. Thus the 2980-2950. Ma assembly of the Isukasia and Kapisilik terranes is distinct from the later 2710-2700. Ma terrane assembly further south in the Nuuk region.

Disciplines

Medicine and Health Sciences | Social and Behavioral Sciences

Publication Details

Nutman, A. P., Bennett, V. C., Friend, C. R. L., Yi, K. & Lee, S. (2015). Mesoarchaean collision of Kapisilik terrane 3070Ma juvenile arc rocks and >3600Ma Isukasia terrane continental crust (Greenland). Precambrian Research, 258 146-160.

Mesoarchaean collision of Kapisilik terrane 3070 Ma juvenile arc rocks and >3600 Ma Isukasia terrane continental crust (Greenland)

Allen P. Nutman[1], Vickie C. Bennett[2], Clark R.L. Friend[3], Keewook Yi[4], Seung Ryeol Lee[5]

Precambrian Research v. 258, p. 146-160 (2015)

[1] GeoQuEST Research Centre, School of Earth & Environmental Sciences, University of Wollongong, Wollongong, NSW 2522, Australia

[2] Research School of Earth Sciences, Australian National University, Canberra, ACT 0200, Australia

[3] Glendale, Tiddington, Oxon, OX9 2LQ, U.K.

[4] Korean Basic Science Institute, Daejeon 305-350, Korea

[5] Korea Institute of Geoscience and Mineral Resources, Daejeon 305-350, Korea

Corresponding author: Allen Nutman, email: anutman@uow.edu.au

Abstract

The Mesoarchaean Kapisilik and Eoarchaean Isukasia terranes in the Nuuk region of southern West Greenland were tectonically juxtaposed in the Archaean. The north of the Isukasia terrane is distal from the Kapisilik terrane and has only rare growth of ~2690 Ma metamorphic zircon and no 2980-2950 Ma metamorphic zircon. The southern part of the Isukasia terrane lies between two ~2690 Ma shear zones, and has locally-preserved high pressure granulite facies assemblages and widespread growth of 2980-2950 Ma metamorphic zircon and also sporadic growth of ~2690 Ma metamorphic zircon. Within this southern part of the Isukasia terrane there is a folded klippe of mylonitised Mesoarchaean detrital meta-sedimentary rocks (carrying >3600 and ~3070 Ma detrital zircons), mafic and ultramafic rocks, with ~2970 Ma metamorphic zircon overgrowths. South of the Isukasia terrane is the Kapisilik terrane, containing ~3070 Ma arc-related volcanic rocks, gabbro-anorthosites and meta-tonalites, intruded by 2970-2960 Ma granites. Zircons of an Ivisârtoq supracrustal belt ~3075 Ma intermediate volcanic rock have initial ε_{Hf} values of +2 to +5 thus are juvenile crustal additions. ~3070 Ma tonalites along the northern edge of the Kapisilik terrane have whole rock positive initial ε_{Nd} values are also juvenile crustal additions. In contrast, igneous zircons in 2960 Ma granites intruded into juvenile ~3075 Ma supracrustal rocks of the Kapisilik terrane have initial ε_{Hf} values of -5 to -10, and must have involved the partial melting of >3600 Ma Isukasia terrane rocks.

The integrated structural and zircon U-Th-Pb-Hf isotopic data show that at 2980-2950 Ma the Kapisilik terrane juvenile arc components collided with, and over-rid, the Isukasia terrane. The southern edge of the Isukasia terrane came to lie in the deep crust under the Ivisârtoq supracrustal belt and melted at 2970-2960 Ma to produce granites. These granites derived from ancient crust rose into the upper crust, where they intruded the overlying allochthonous juvenile ~3075 Ma Ivisârtoq supracrustal belt arc assemblages. The southern edge of the Isukasia terrane is interpreted as an interior nappe of Eoarchaean basement rocks interfolded with a klippe of Mesoarchaean metasedimentary and mafic/ultramafic rocks, both of which are affected by 2980-2950 Ma metamorphism. The mixed Eoarchaean-Mesoarchean detrital provenance suggests that the klippe could be dismembered components of an accretionary prism or forearc crust. The northern part of the Isukasia terrane is interpreted as foreland, free of 2980-2950 Ma high-grade metamorphic overprint. This shows that the Isukasia terrane is not a coherent block, but contains ancient rocks that are parautochthonous or allochthonous to each other, with contrasting later metamorphic history.

At ~2690 Ma the crustal architecture arisen from Mesoarchaean collision between an older continental block and an island arc was reworked along intra-crustal shear zones, coeval with amphibolite facies metamorphism. This reworking followed on from major terrane assembly at 2710-2700 Ma in the southern part of the Nuuk region, when the Eoarchaean Færingehavn terrane was juxtaposed with 2840-2825 Ma arc rocks. Thus the 2980-2950 Ma assembly of the Isukasia and Kapisilik terranes is distinct from the later 2710-2700 Ma terrane assembly further south in the Nuuk region. (499 words)

Keywords: Isukasia terrane; Ivisârtoq supracrustal belt; Mesoarchaean collisional orogeny; Archaean tectonics; crustal remelting

1. Introduction

Archaean gneiss complexes are now regarded to contain distinct terranes with their own early evolution (tectonostratigraphic terranes *sensu* Coney, 1980) that were later assembled to have a later common tectonothermal history for all terranes (Friend et al., 1987, 1988, 1996, Friend and Kinny, 2001; Crowley, 2002). However, the collages of terranes that comprise Archaean gneiss complexes can have hidden within them evidence of several unrelated terrane assembly events. This is similar to the structure within Phanerozoic orogens where sequential events can be recognised, with some of the individual terranes showing their own internal tectonothermal evolution. As an example, the Cenozoic European Alps formed as a result of several terrane assembly events, and some of the basement massifs reveal a history of earlier Hercynian events (e.g., Zeck and Williams, 2001).

In this paper we explore the situation of superimposed Archaean terrane assembly events in the north-eastern Isukasia-Ivisaartoq part of the Nuuk region gneiss complex in southern West Greenland (Fig. 1). In this part of the complex, Eoarchaean rocks of the Isukasia terrane lie to the north and east of Mesoarchaean rocks of the Kapisilik terrane (Hall and Friend, 1979; Chadwick, 1985, 1990; Friend and Nutman, 2005). Mapping, structural studies, metamorphic petrology and zircon U-Th-Pb-Hf isotopic data reveal a history of Mesoarchaean collision between the Isukasia terrane (an old continental massif) and >3000 Ma components of the Kapisilik terrane (a juvenile arc). We argue that the architecture of the Mesoarchaean orogen was reworked by superimposed Neoarchaean intra-crustal shearing. Similarities and differences between this Mesoarchaean orogen and Phanerozoic collisional orogens are discussed.

2. Previous tectonic interpretations in Isukasia – Ivisaartoq area

Prior to the recognition in the Nuuk region of tectonostratigraphic terranes and their folded mylonite boundaries, Hall and Friend (1979,1983) and Chadwick (1985, 1990) undertook studies of the tectonothermal evolution of the Isukasia-Ivisaartoq part of the Nuuk region. Because the terrane boundaries were not recognised, fold structures were hard to decipher, because it was not realised that some major closures were internal to a particular terrane, and could not be traced into an adjacent terrane. The continuity of fold style across the region was the accepted way of interpreting these structures, as shown on the 1:500,000 scale geological map of the region (Allaart, 1982; Kalsbeek and Garde, 1989). However, an important early observation was that the Eoarchaean rocks of what is now recognised as the Isukasia terrane are structurally below the Mesoarchaean rocks of the Ivisaartoq area (Chadwick, 1990) that led to our recognition that the Eoarchaean Itsaq Gneiss Complex occurs in two tectonic slices - the Færingehavn and Isukasia terranes (Friend and Nutman, 2005). The Mesoarchaean rocks of the Ivisaartoq area are now assigned to the Kapisilik terrane (Friend and Nutman, 2005; Fig. 1).

Another handicap for the early studies was the dearth of accurate and precise geochronology, such that all tectonothermal events affecting both the Eoarchaean Isukasia terrane and the Mesoarchaean Kapisilik terrane could only be placed within ~450 million years – between ~3000 Ma (the age for regional Mesoarchaean gneisses; e.g., Baadsgaard and McGregor, 1981) and ~2560 Ma (the age for the late-kinematic Qôrqut granite complex; e.g., Baadsgaard, 1976).

In the first regional tectonic synthesis since the recognition of the tectonostratigraphic terranes, McGregor et al. (1991) implicitly regarded terrane assembly and all major tectonic events in the Isukasia – Ivisaartoq area to be Neoarchaean, in accordance with the recognition in the south of the Nuuk region that assembly of the >3600 Ma Færingehavn, 2840-2820 Ma Tre Brødre and the 2920-2800 Ma Tasiusarsuaq terranes occurred in the Neoarchaean. The evolution and assembly of these three terranes has been studied in detail, with integrated whole rock geochemistry, zircon U-Pb-Hf and whole rock Nd data showing that these terranes contain mostly juvenile TTG rocks with mutually exclusive ages (Nutman et al., 1989; Friend et al., 1986, 2009; Næraa et al., 2007). Integrated metamorphic petrology and zircon U-Pb dating and trace element geochemical studies indicate that these disparate terranes were assembled from ~2720 Ma onwards, with early tectonothermal histories within each terrane overprinted by tectonothermal events following terrane assembly (Friend et al., 1987; 1996; Nutman et al., 1989; Nutman and Friend, 2007; Crowley, 2002; Dziggel et al., 2014). However, Hanmer et al. (2002) argued that terrane assembly in the Isukasia area took place at ~3000 Ma, and previous interpretations of Neoarchaean terrane assembly elsewhere in the Nuuk region was in error. This suggestion is not compatible with the Tre Brødre and Tasiusarsuaq terranes being dominated by rocks with ages of 2850-2800 Ma (e.g., Crowley, 2002; Næraa et al., 2007; Friend et al., 2009). Friend and Nutman (2005) confirmed that terrane assembly in the Isukasia to Ivisaartoq area had indeed occurred in the Mesoarchaean (~2950 Ma) and, was an event unrelated to the Neoarchaean (≤2720 Ma) assembly of the Færingehavn, Tre Brødre and Tasiusarsuaq terranes in the south.

3. Analytical methods and data interpretation

3.1. SHRIMP zircon U-Pb isotopic data

The new zircon U-Pb data were obtained with SHRIMP-RG instrument of the Australian National University and the SHRIMP-2 instrument at the Korean Basic Science Institute. The selected separated zircons were hand-picked under a binocular microscope and were mounted with Temora or FC1 reference zircons and cast in epoxy resin plugs. The cured plugs were ground and polished to expose the unknown zircon mid sections at the surface. Cathodoluminescence (CL) images were acquired of the zircons in order to select the least damaged domains for analysis. A 20-25 μm spot was used for analysis. $^{238}U/^{206}Pb$ in the unknowns was referenced to Temora or FC1 (considered concordant in the U-Pb system with an ages of 417 and 1099 Ma respectively; Black et al., 2003; Paces and Miller, 1993) and U was calibrated against fragments of the reference zircon crystal SL13 (238 ppm U) located in a set-up mount.

Geochronological information comprises new data (samples G05/26, G91/82, G03/75, G04/05 and G12/165 in Table 1) together with samples 200892, 200499, MR81/318, G91/68, G91/92, G93/86, G93/88, G97/04, G97/58 (from Nutman and Collerson, 1991; Nutman et al., 2002, 2004a; Friend and Nutman, 2005). All relevant ages are summarised in Figure 2. Assessment of rock ages or components within them is based on $^{207}Pb/^{206}Pb$ weighted means of analysis of sites discriminated on the basis of CL petrography, with near concordant $^{207}Pb/^{206}Pb$ and $^{206}Pb/^{238}U$ ages and low content of common Pb. Calculations and graphical presentation of data were undertaken using ISOPLOT (Ludwig, 2003).

3.2. LA-MC-ICPMS Lu-Hf analytical method

Zircon hafnium isotopic compositions were determined over two analytical sessions at Research School of Earth Sciences, ANU, using a ThermoFinnigan Neptune multi-collector ICPMS coupled to a ArF λ=193 nm eximer laser ablation system following methods described by Hiess et al. (2009). In session 1, the laser was focused to a 47 μm diameter spot and pulsed at 5 Hz with an energy density at the sample surface of ~5 J/cm^2. In session 2, the conditions varied slightly; the laser was focused to a 41 μm spot and pulsed at 7 Hz with an surface energy density of ~5 J/cm^2, and jet sample cones were used in place of standard cones to enhance sensitivity. ^{171}Yb, ^{173}Yb, ^{174}Hf, ^{175}Lu, ^{176}Hf, ^{177}Hf, ^{178}Hf, ^{179}Hf and ^{181}Ta isotopes were simultaneously measured in static-collection mode on 9 Faraday cups with 10^{11} Ω resistors. A large zircon crystal from the Monastery kimberlite was used to tune the mass spectrometer to optimum sensitivity. Analysis of a gas blank and a suite of secondary reference zircons (Mud Tank, 91500, Temora-2, FC1 and QGNG) were performed systematically after every 10-12 sample spot analyses.

Data were acquired in 1 s integrations over 100 s or until the grain burned through. When possible the larger diameter laser spot was placed over the SHRIMP analysis spot. Offline segmental processing of the laser ablation data allowed detection of any down-hole variation in Lu/Hf and ^{176}Hf/^{177}Hf related to drilling through different growth zones. During data reduction on a custom Excel™ spreadsheet, time slices were cropped to periods maintaining steady ^{176}Hf/^{177}Hf signals. In the analyses presented in Table 2, Lu/Hf and ^{176}Hf/^{177}Hf ratios were uniform throughout data acquisition. Data reduction incorporated a within run dynamic amplifier correction. Total Hf signal intensity typically fell from >12 to 6 volts during a single analysis.

The measured $^{178}Hf/^{177}Hf$, $^{176}Lu/^{177}Hf$ and $^{176}Hf/^{177}Hf$ ratios with 2σ uncertainties for the sample analyses are presented in Table 2 and the data for the reference zircons for each analytical session are given in the Appendix Table A1. Mass bias was corrected using an exponential law (Russell et al. 1978; Chu et al. 2002; Woodhead et al. 2004) and a composition for $^{179}Hf/^{177}Hf$ of 0.732500 (Patchett et al. 1981). Yb and Lu mass bias factors were assumed to be identical and normalized using an exponential correction to a $^{173}Yb/^{171}Yb$ ratio of 1.129197 (Vervoort et al. 2004). The intensity of the ^{176}Hf peak was determined accurately by removing isobaric interferences from ^{176}Lu and ^{176}Yb. Interference-free ^{175}Lu and ^{173}Yb were measured and the interference peaks subtracted according to reported $^{176}Lu/^{175}Lu$ and $^{176}Yb/^{173}Yb$ isotopic abundances of Vervoort et al. (2004). As a quality check of these procedures, $^{178}Hf/^{177}Hf$ and $^{174}Hf/^{177}Hf$ ratios for all zircon reference materials and samples are reported (Table A1). Average measured $^{176}Lu/^{177}Hf$ ratios within the reference zircons (Table A1) are in good agreement with the solution values reported by Woodhead and Hergt (2005) of 0.000009, 0.000311, 0.001090 and 0.001262 respectively.

The mean $^{176}Hf/^{177}Hf$ ratios for each of the reference zircons for each session deviate from published solution values of Woodhead and Hergt (2005) by <0.2 ε_{Hf} units for session 1 and <0.4 for session 2 (Appendix Table A1)). No correlation exists between $^{176}Hf/^{177}Hf$ and $^{178}Hf/^{177}Hf$, $^{174}Hf/^{177}Hf$ or $^{176}Lu/^{177}Hf$ ratios for any zircon reference materials, including the high Lu/Hf zircons, Temora-2 and FC1, indicating that calculations for mass bias and Yb interference corrections were applied accurately. For the unknown zircons, initial $^{176}Hf/^{177}Hf$ ratios for each spot were calculated using their the SHRIMP U-Pb age for the rock, present day CHUR compositions of $^{176}Hf/^{177}Hf = 0.282785\pm11$, $^{176}Lu/^{177}Hf = 0.0336\pm1$ (Bouvier et al.

2008), and a ^{176}Lu decay constant of 1.867±8 x10^{-11}y^{-1} (Scherer et al. 2001; Söderlund et al. 2004).

Several sources of uncorrelated error may exist within these LA-MC-ICPMS analyses that do not account for the external scatter seen in some reference zircons (e.g. Temora and FC1). Therefore, a conservative approach is taken to estimate the absolute uncertainty of each spot that is used to calculate weighted mean ε_{Hf} compositions. Within-run errors determined for individual zircon analyses are summed in quadrature with an estimate of external reproducibility from the zircon reference materials for each analytical session. As all zircons are from single crystallisation age populations, initial Hf isotopic compositions are calculated using the best age estimate from the pooled SHRIMP U-Pb data.

4. Integrated structural observations and zircon-monazite isotopic data

4.1. Northern Isukasia terrane

The northern part of the Isukasia terrane is bounded to the south and west by a Neoarchaean mylonite zone that can be traced around a regional Neoarchaean antiform (mylonite-1, Fig. 1). Throughout much of the northern part of the Isukasia terrane discordances are preserved between the ~3500 Ma Ameralik dykes and structures in their host rocks (Fig. 3A). This demonstrates that post-Eoarchaean strain has been weak in that area (Bridgwater and McGregor, 1974; Nutman, 1984; Nutman et al., 1996). To the south towards mylonite-1 strain increases, such that the Ameralik dykes become more deformed and discordances are reduced.

North of the Isua supracrustal belt (central gneisses in Fig. 1), titanite in the Eoarchaean rocks has U-Pb ages of ~3600 Ma (Crowley et al., 2002). Throughout the northern part of the Isukasia terrane post-3400 Ma metamorphic zircon is rare (data in Nutman et al., 1996, 1997, 2000, 2002, 2007; Nielsen et al. 2002; Crowley et al., 2002). This indicates only modest heating (≤550°C) in post- Ameralik dyke events, in accord with the development of epidote amphibolite facies assemblages. Consequently, Ameralik dykes north of the Isua supracrustal belt are weakest-deformed and usually preserve their igneous microgabbroic textures, with relicts of igneous plagioclase and more rarely pyroxene set in reaction haloes of more sodic plagioclase + epidote + amphibole ± chlorite (Nutman, 1986). Southwards into the Isua supracrustal belt the dykes become more deformed and, starting at their margins, start to develop a hornblende lineation (Nutman, 1986). This demonstrates that there was epidote amphibolite facies metamorphism synchronous with partitioned ductile deformation, after all the Ameralik dykes were intruded. Based on cross-cutting relationships, the youngest Ameralik dykes trend north-south (Nutman, 1986). Zircon U-Pb geochronology was undertaken on a north-south dyke to constrain the *maximum* age of the post-dyke ductile deformation and metamorphism. A dyke was sampled just north of the Isua supracrustal belt (sample G05/26 on Fig. 1). At 65°06.42'N 49°58.14'W this dyke contains felsic patches that were residual melts in the crystallisation of the mafic magma. Zircons in this sample would comprise new magmatic grains grown at the time of dyke emplacement. The sample G05/26 yielded stubby prismatic zircons that are yellow to deep brown in colour and generally appear dull in CL images with irregular domains indicating recrystallisation. The Th, U and Th/U of the zircons are high (Table 1), typical of zircons associated with mafic magmas. $^{206}Pb/^{238}U$ and $^{207}Pb/^{206}Pb$ ratios show large errors well beyond those expected from counting statistics alone, due to the heterogeneity in the target sites leading to fluctuation in ion counting rates during data acquisition. The U-Pb data scatter across Concordia, with some showing ≥20% normal discordance, and some showing up to 20% reverse discordance (Fig. 4A, Table 1). The former indicates loss of radiogenic Pb from damaged lattices and the latter is due to a matrix contrast between the high Th+U G05/26 zircons versus the much lower Th+U reference FC1 standard zircons. This matrix effect causing fractionation of the secondary ions is revealed by a difference in $^{238}U^{16}O/^{238}U^{+}$ for the G05/26 zircons (average 8.00±0.18) versus the FC1 standard zircons (average 6.99±0.06). Due to the errors introduced into determination of $^{206}Pb/^{238}U$ in the G05/26 zircons, most reliance is placed on ages derived from the $^{207}Pb/^{206}Pb$ ratios, which are free of this instrumental fractionation effect. $^{207}Pb/^{206}Pb$ ratios scatter beyond analytical error, but have the highest density between 2800-2750 Ma. Based on this data, an accurate and precise age for timing of emplacement of the Ameralik dyke cannot be obtained. However the results do indicate it is most probable that the dyke was intruded between 2800-2750 Ma, which is significantly younger than the age of ~3510 Ma (Nutman et al., 2004b) obtained for the more abundant east-west trending dykes, that are older based on cross-cutting relationships. A 2800-2750 Ma age for this dyke indicates that the superimposed epidote amphibolite facies metamorphism must be younger, and occurred in the Neoarchaean. The tail of apparent $^{207}Pb/^{206}Pb$ ages <2750 Ma (Fig. 4A) reflects partial loss of radiogenic Pb in younger tectonothermal events.

In the central part of the Isua supracrustal belt in a Neoarchean higher strain domain, some zircons in metaquartzite sample MR81/318 have 2696±6 Ma low Th/U metamorphic overgrowths (Fig. 1; Nutman and Collerson, 1991). Farther to the south there is a decrease in epidote and the local appearance of garnet in the Ameralik dykes. This is accompanied by the development of a hornblende lineation in them (Nutman, 1986). This suggests a southerly increase in post-Ameralik dyke metamorphic grade as well as strain. South of the Isua supracrustal belt, sample G97/04 of a late Eoarchaean pegmatite (Fig. 1) contains Neoarchaean monazites. The monazite $^{207}Pb/^{206}Pb$ ages scatter beyond analytical error (data in Friend and Nutman, 2005), from which populations of 2674±9 Ma and 2656±12 Ma are resolved. From the same area, Crowley (2003) reported titanite ages of ~2650 Ma in Eoarchaean rocks. Thus between the Isua supracrustal belt and mylonite 1 there is diverse mineralogical evidence for a Neoarchaean thermal event. In contrast, throughout the part of the Isukasia terrane north of mylonite-1, Mesoarchaean (2980-2950 Ma) U-Pb mineral ages have not been reported.

4.2. Mylonite-1, the tectonic boundary between the northern and southern parts of the Isukasia terrane

A post Ameralik dyke mylonite with superimposed metamorphism locally up to ~100 m wide separates the northern and southern parts of the Isukasia terrane (mylonite-1, Fig. 1). In the northern part of the Isukasia terrane approaching this mylonite, there is a distinct post Ameralik dyke (<3500 Ma) gradient of increasing strain. The mylonite is dominated by homogeneous, fine-grained, biotite-foliated quartzo-feldspathic rocks, but with some domains showing rootless folds described by discontinuous bands of pegmatitic material. Zircon dating of this mylonite has been undertaken at two localities. Sample G97/58 (Fig. 1) yielded low Th/U metamorphic zircons with a weighted mean $^{207}Pb/^{206}Pb$ age of 2686±5 Ma (Nutman et al., 2002). To the southwest, sample G91/82 (Fig. 1) of similar homogeneous quartzo-feldspathic metamylonite with low Th/U metamorphic zircons with close to concordant U-Pb ages yielded a $^{207}Pb/^{206}Pb$ weighted mean age of 2688±9 Ma (Fig. 4B, Table 1). Northwards, mylonite-1 is excised by later Neoarchaean upper greenschist facies shear zones that are the northern extension of the ~2540 Ma (Nutman et al., 2010) Ivinguit fault in the Nuuk-Godthåbsfjord area. However, structures in this area are further disrupted by the Proterozoic Ataneq Fault (e.g. Park, 1987). To the east towards the Inland Ice, mylonite-1 has not been positively mapped. However, based on regional foliation trends, its extrapolated position towards the Inland Ice is portrayed in Figure 1.

4.3. Southern Isukasia terrane

The area between mylonite-1 and mylonite-2 (Fig. 1) is dominated by Eoarchaean rocks of the Isukasia terrane that were strongly deformed after emplacement of the Ameralik dykes. Therefore, discordances between the Ameralik dykes and structures in their host Eoarchaean rocks are much rarer than in the northern part of the terrane. The Ameralik dykes can also be disrupted by pegmatite veins (Fig. 3B), a feature that is very rare in the northern part of the terrane. Furthermore, the Ameralik dykes describe isoclinal closures, and commonly carry metamorphic garnet, or have amphibole + plagioclase symplectites replacing garnet. Supracrustal rocks within this southern part of the Isukasia terrane are commonly garnetiferous and locally, preserved within mafic rocks, there are relict high-pressure granulite facies assemblages (garnet + clinopyroxene + plagioclase + quartz; Fig. 3C at 64°58.65'N 49°56.85'W). However, such assemblages have been widely retrogressed under epidote amphibolite facies conditions, such that selvedges of hornblende occur between garnet and clinopyroxene, and there is widespread alteration of calcic plagioclase to zoisite + albite (Fig. 3C).

Units of supracrustal rocks, metagabbros and ultramafic rocks describe folds internal to the southern part of the Isukasia terrane, with fold axial traces of closures within amphibolite units approximately parallel to the bounding mylonites 1 and 2

(Fig. 1). This is most evident in aeromagnetic coverage of the region (Rasmussen and Thorning, 1999). The aeromagnetic signatures suggest that these early structures swing over the regional Neoarchaean antiform in the west (Fig. 1), and are attenuated in the western limb. Rocks in the western limb of the Neoarchaean antiform are strongly deformed, and contain early isoclinal folds dismembered by later ductile deformation.

Previous zircon U-Pb geochronological studies have documented the widespread development of Mesoarchaean (2980-2950 Ma) low Th/U metamorphic zircon in the southern part of the Isukasia terrane (Fig. 1). Metamorphic zircons with these ages are reported from Eoarchaean orthogneisses and supracrustal rocks in the eastern part (Nutman et al., 2002; Friend and Nutman, 2005), and in the attenuated western limb of the Neoarchaean antiform (data in Hanmer et al., 2002). New data is reported here from a garnetiferous schist G12/165 in the east of the area (64°58.64'N 49°56.78'W) close to the relict high pressure granulite assemblage illustrated in Figure 3C. The protolith of this garnetiferous schist was probably a mafic to intermediate volcanic rock or clay rich sediment derived from such sources, which would be compatible with the lack of volcanic zircons within it. It yielded abundant low Th/U metamorphic zircons (Table 1) of mostly equant habit and appearing homogeneous or with sector zoning in cathodoluminescence images. Most sites yielded close to concordant U-Pb ages (Fig. 4C). The $^{207}Pb/^{206}Pb$ ages spread beyond analytical error, with a weak bimodality apparent in their distribution. A main group with a weighted mean $^{207}Pb/^{206}Pb$ age of 2970 ± 4 Ma (MSWD=0.88) is equated with peak metamorphism, probably reflected in the nearby relict high pressure granulite assemblages. A lesser, slightly younger group is apparent, with a possible weighted mean $^{207}Pb/^{206}Pb$ age of 2943 ± 9 Ma (MSWD=0.68), perhaps reflecting the amphibolite facies retrogression of the peak high pressure assemblage.

4.4. Mesoarchaean supracrustal rocks intercalated with the southern Isukasia terrane

Within the southern part of the Isukasia terrane are belts of supracrustal, gabbroic and ultramafic rocks. Some of these are definitely Eoarchaean in age, because they occur as trains of enclaves within surrounding ~3800 Ma tonalitic orthogneisses (Nutman et al., 1996). However, also present are bodies of supracrustal and mafic rocks that are not disrupted by the adjacent Eoarchaean gneisses, which occur in early fold cores. In the eastern part of the region, a synformal fold core consists of quartzo-feldspathic schists, amphibolites and ultramafic rocks (G93/86 locality, Fig. 1). Its contact with the underlying Eoarchaean gneisses is sharp, and is interpreted as a metamorphosed mylonite. Zircon U-Pb dates for quartzo-feldspathic schist G93/86 were reported by Nutman et al. (2004a). Protolith zircons of sedimentary and possibly volcanic origin have ages from ~3800 to 3000 Ma. <3100 Ma grains show a dominant ~3070 Ma population, and a lesser number of ~3050 Ma grains (Nutman et al., 2004a). Overgrowths and whole grains which appear dull in CL images and with higher U content and lower Th/U ratios yielded a weighted mean $^{207}Pb/^{206}Pb$ age of 2968 ± 10 Ma (Nutman et al., 2004a). These sedimentary rocks were deposited after ~3050 Ma (youngest detrital grains) but before 2968 Ma (high grade metamorphism), thus are clearly younger than the Eoarchaean Isukasia terrane. We interpret them and their associated mafic and ultramafic rocks as a tectonic klippe overlying the Isukasia terrane, that was folded and first metamorphosed at ~2970 Ma.

4.5. Mylonite-2, the tectonic boundary of the Isukasia and Kapisilik terranes

Mylonite-2 forms the boundary between the Eoarchaean rocks of the Isukasia terrane to the north and a diverse assemblage of Mesoarchaean rocks of the Kapisilik terrane to the south (mylonite-2, Fig. 1). The mylonite has been traced continuously from the edge of the Ice Cap at the north-eastern edge of the Ivisârtoq supracrustal belt, to the western limb of the Neoarchaean antiform, where it is truncated by the northern continuation of the Ivinguit fault (Fig. 1). The foliation in the rocks on either side of the mylonite is parallel with it, but on a larger scale the mylonite truncates early folds within the Kapisilik terrane (Fig. 1). The mylonite consists of foliated biotite schists, commonly with the development of tectonised pegmatite within it. Reconnaissance zircon U-Pb dating was undertaken on a Kapisilik terrane gneiss in the southern edge of the mylonite (sample G93/88, Fig. 1; Friend and Nutman, 2005). The sample is flaggy foliated gneiss with concordant synkinematic pegmatite bands. Two types of zircon were encountered. Mesoarchaean grains with low U (<300 p.p.m.) and high Th/U (>0.3) and ones with higher U (>2000 p.p.m.) and lower Th/U (<0.1; Table 1). Both populations show variable amounts of ancient loss of radiogenic lead, displayed by dispersion in $^{207}Pb/^{206}Pb$ beyond analytical error (Fig. 4D). Assuming those with the oldest apparent ages are the least disturbed, the low U, higher Th/U zircons have a mean age of 3072 ± 14 Ma, and the high U, low Th/U zircons have a mean age of 2680 ± 5 Ma. These are interpreted as the age of the Kapisilik terrane tonalitic protolith and of the synkinematic pegmatite bands respectively. 3072 Ma agrees well with an age of 3070 ± 9 Ma for Kapisilik terrane tonalite G91/92 further to the west and 3075 ± 15 Ma for felsic volcanic rock GGU2000892 in the Ivisârtoq supracrustal belt to the east (Fig. 1; Friend and Nutman, 2005). 2680 ± 5 Ma agrees with ages of 2688 ± 9 and 2689 ± 5 Ma for metamorphic zircons within mylonite-1 (Fig. 1).

4.6. ~3070 Ma arc rocks in the northern Kapisilik terrane

Zircon U-Pb dates of 3075-3070 for the volcanic rocks of the Ivisârtoq supracrustal belt and tonalitic gneisses of the northern margin of the Kapisilik terrane were presented by Friend and Nutman (2005). Detailed whole rock geochemical studies of the Ivisârtoq supracrustal belt shows that the amphibolites within it have trace element signatures typical of juvenile arc-related tholeiites, picrites and boninites indicating fluid-fluxing of the mantle in a supra-subduction zone setting plus MORB indicating some oceanic crust (Jenner, 2006; Polat et al., 2007; Ordóñez-Calderón, 2009). The juvenile nature of these rocks is also indicated by the whole rock high positive initial ε_{Nd} values up to +5 for mafic volcanic rocks, diorites and ~3070 Ma tonalites in the northern edge of the Kapisilik terrane (Polat et al., 2008; Bennett, unpublished data).

Hf isotopic analyses are presented for the high Th/U 3075 Ma magmatic zircons of the Ivisârtoq supracrustal belt volcanic rock GGU200892 (Table 2, Fig. 5). The 13 analysed grains have a narrow range of measured $^{176}Hf/^{177}Hf$ (with ε_{Hf}= -67.1 to -63.6). The initial compositions calculated at the 3075 Ma crystallisation age all lie above chondritic mantle compositions with positive ε_{Hf} (3075) values = +4.6 to +2.1 and requires felsic volcanic rock GGU200892 to have formed from a juvenile mantle source with no contributions from older crustal materials. This is a similar ε_{Hf} range as observed in some other Mesoarchean mantle and mantle-derived rocks, as for example ~ 3000 Ma oceanic basalts in the Tartoq Group, SW Greenland (Szilas et al., 2013), with initial ε_{Hf} values of ~ +4.

4.7. ~2970 Ma granites in the northern Kapisilik terrane

Pale, non-porphyritic granite/granodiorite was intruded into the Ivisârtoq supracrustal belt to form the *central Ivisârtoq dome* (Fig. 1; Hall and Friend, 1983; Chadwick, 1985). Within the eastern part of the dome these granitic gneisses contain enclaves of gneisses cut by mafic dykes and then partially melted (Hall and Friend, 1983). Due to the presence of the dyke remnants, these enclaves have been interpreted as Eoarchaean gneisses of the Itsaq Gneiss Complex (formerly known as *Amîtsoq gneisses* in Hall and Friend, 1983). Magmatic zircons in sample GGU200499 of the granite have yielded a weighted mean $^{207}Pb/^{206}Pb$ age of 2961 ±11 Ma (Friend and Nutman, 2005). On the western limb of the regional Neoarchaean antiform shown on Figure 1, granitic/granodioritic gneisses are also encountered in the edge of the Kapisilik terrane. South of 65°N these are homogeneous, and magmatic zircons from sample G91/83 has yielded a weighted mean $^{207}Pb/^{206}Pb$ age of 2972 ±12 Ma (Fig. 1; Garde et al., 2001). North of 65°N, these homogeneous granitic gneisses grade into migmatites, consisting of granitic neosome invading an older suite of gneisses cut by amphibolitised, deformed mafic dykes (Fig. 2D), suggestive of Itsaq Gneiss Complex rocks cut by Ameralik dykes. This resembles the field relationships seen in the central Ivisârtoq dome, but with stronger superimposed ductile deformation.

Hf isotopic analyses have been undertaken on the magmatic 2970-2960 Ma zircons from granite samples GGU200499 and G91/83 (Table 2, Fig. 5). The 14 analysed zircons from GGU200499 yielded a narrow range of measured ε_{Hf} values (from -70.8 to -74) reflecting a single Hf population and with negative initial ε_{Hf} values (at 2961 Ma) of -8.1 to -5.5 with a mean of -6.4± 0.8. The 14 analysed grains from G91/83 have measured ε_{Hf} from -81.2 to -70.7 and with initial ε_{Hf} vales (at 2972 Ma) of -15.1 to -3.8 to. The strongly negative ε_{Hf} values for both of these Mesoarchean samples require their derivation largely or totally from older, Eoarchaean felsic (low $^{176}Lu/^{177}Hf$) sources. A minimum age estimate of the average crustal sources of these samples of ~3500 Ma, is provided from single stage model age calculations (Table 2). More realistic 2-stage model ages, where the first stage is $^{176}Hf/^{177}Hf$ evolution in a felsic source prior to melt extraction and zircon formation in the Mesoarchean, gives source ages of 3600 to 3900 Ma, in accord with known ages of basement rocks of the Itsaq Gneiss Complex (Nutman et al., 1996, 2013).

4.8. Neoarchaean mylonite-3, the southern edge of the Kapisilik terrane in northern Godthaabsfjord

On southwestern Ivisaartoq, in the core of a Neoarchaean synform (Fig. 1), the Kapisilik terrane is overlain by ~2800 Ma rocks presently correlated with the Tre Brødre terrane plus the Eoarchaean Færingehavn terrane in the south of the Nuuk region (Friend and Nutman, 2005). The boundary with the underlying Kapisilik terrane is mylonite-3 affected by Neoarchaean folding, and is exposed on the southern shore of Ivisaartoq. The position of mylonite-3 to the west is less certain, because its trace runs through inland areas that were systematically mapped prior to the recognition of tectonostratigraphic terranes in the region (Chadwick and Coe, 1988). Our knowledge of it comes from a detailed coastal transect plus a few inland helicopter stops to collect samples for reconnaissance zircon U-Pb geochronology (Fig. 1).

G91/68 (Fig. 1) is a 2710±13 Ma diatexite developed in >3600Ma Itsaq Gneiss Complex (data in Friend et al., 1996; Friend and Nutman, 2005). Inland to the northwest at GPS 64°48.97'N 50°24.76'W, a body of granite (sample G04/05; Fig. 1) was emplaced into a fold interference structure described by an amphibolite unit. The zircons in this sample are mostly magmatic oscillatory-zoned prisms, with a few inherited cores. The main igneous population of zircons has moderate to high U abundance (>300 p.p.m.) and U-Pb ages that are concordant within error (Table 1; Fig. 4E). They yield a weighted mean $^{207}Pb/^{206}Pb$ age of 2707 ± 7 Ma (MSWD=0.44) that is interpreted as the crystallisation age of the granite. The majority of the inherited cores have ages of ~3000 Ma. Two analyses of the core in grain 9 have ages >3860 Ma (Table 1; off-scale in Fig 4E). Further north migmatitic gneisses are represented by sample G03/75 (Fig. 1). Only nine reconnaissance zircon U-Pb measurements were undertaken on this sample (Table 1, Fig. 4F). Oscillatory-zoned grains with lower U content (<300 p.p.m.) and with Th/U (>0.3) yield the oldest ages, but with $^{207}Pb/^{206}Pb$ scattering beyond analytical error. On the basis that this is due to some variable loss of radiogenic Pb in ancient times, those with the oldest apparent ages yield a weighted mean $^{207}Pb/^{206}Pb$ age of 2993 ± 12 Ma. A group of analyses that yielded Neoarchean ages are of high U (>900 p.p.m.) low Th/U (<0.1) also have $^{207}Pb/^{206}Pb$ that scatter beyond analytical error (Fig. 4F). Applying the same radiogenic Pb-loss model, those with the oldest apparent ages yield a weighted mean $^{207}Pb/^{206}Pb$ age of 2721 ± 4 Ma.

The position of mylonite-3 can be extrapolated to the west and north from Ivisaartoq by following mapped foliation trends and mimicking the path of mylonites 1 and 2 to the north as they are folded around regional Neoarchaean structures. This would place the inferred position for mylonite-3 between rocks in the northwestern

Kapisilik terrane that have *no* evidence of tectonothermal events and granite emplacement at 2720-2700 Ma and those to the south and west that *all* show these events (Fig. 1). In the north, this links with a mylonite recognised by Nutman in a (1982) regional mapping programme. All three mylonites are truncated by a later fault that is the northerly continuation of the Ivinguit fault in Godthåbsfjord (Friend et al., 1996).

5. Discussion

5.1. ~2970 Ma collisional orogeny along the southern margin of the Isukasia terrane

Integrated structural, metamorphic, zircon U-Pb geochronology and radiogenic isotopic data can be used to reconstruct crustal evolution at 2980-2950 Ma (Fig. 6). The 3075-3070 Ma Ivisârtoq supracrustal belt and associated tonalites display whole-rock geochemical and Nd, Hf radiogenic evidence that they represent juvenile crust at the time that they formed (data in this paper and Polat et al., 2007). The favoured environment for the formation of this juvenile crust at ~3070 Ma is analogous to modern island arc settings, distal from continental influence (Fig. 6A; Garde, 2007; Polat et al., 2007). Tonalites from elsewhere in the Kapisilik terrane have yielded Mesoarchaean ages between 3070 and 3000 Ma, indicating continuing construction of a juvenile arc complex (Fig. 6B). A similar scenario is mirrored in the neighbouring Mesoarchaean Akia terrane to the west (Garde et al., 2001).

Between mylonites 1 and 2, the southern part of the Isukasia terrane is overlain by a klippe of Mesoarchaean quartzo-feldspathic schists, amphibolites and ultramafic rocks. The schists contain both Eoarchaean (>3600 Ma) and Mesoarchaean (~3070 and 3050 Ma) detrital grains. Hence, despite the allochthonous nature of these supracrustal rocks, they received detritus from sources the same age as juvenile components in the Kapisilik terrane to the south and the underlying Isukasia terrane. They might represent an assemblage (accretionary prism or forearc setting?) formed just prior to collision of the Isukasia terrane and the Mesoarchaean arc in the Kapisilik terrane (Fig. 6B).

The juvenile arc rocks of Ivisaartoq are structurally underlain in the central Ivisârtoq dome by 2970-2960 Ma granites/granodiorites formed by partial melting of Eoarchaean orthogneisses (Fig. 6C). Following subsequent development of 2690 Ma shear zones and folding, these granites now occur at the edge of the Kapisilik terrane, with the Ivisârtoq supracrustal belt forming a carapace over it (Fig. 6D). A similar scenario is also evident in the western part of the region, where 2972 Ma granodiorite G91/83 was also produced by the melting of Eoarchaean crust, and this granodiorite can be traced north into a heterogeneous domain of neosome and palaeosome containing disrupted amphibolite dykes (probably Eoarchaean rocks; Fig. 2D). Thus by 2970 Ma, the juvenile 3075-3070 Ma crust had come to overlie Eoarchaean crust, probably the southern edge of the Isukasia terrane (Fig. 6C).

The southern part of the Isukasia terrane is strongly affected by high-grade metamorphism at 2970-2940 Ma, as shown by the widespread growth of low Th/U metamorphic zircon at that time. Structural trends (Chadwick and Coe, 1988) and aeromagnetic signatures (Rasmussen and Thorning, 1999) indicate that this part of the terrane contains an early large nappe-like closure that is folded over the Neoarchaean antiform in the west of the area (Fig. 1). Furthermore, amphibolites in this terrane widely develop garnet, although it has commonly been replaced by hornblende + plagioclase symplectites during subsequent retrogression. There are locally-preserved relict high pressure granulite facies assemblages in mafic rocks, albeit they have been widely retrogressed under epidote amphibolite facies conditions (Fig. 3C). This suggests transient high pressure metamorphism, probably at ~2970 Ma. The Eoarchaean rocks of the southern Isukasia terrane are overlain by one or more klippe of Mesoarchaean supracrustal rocks, now preserved in synformal fold noses (Fig. 6D). These might be remnants of allochthonous Mesoarchaean crust that overrode the Isukasia terrane. The assembled data suggests that the southern Isukasia terrane represents a basement complex that at ~2970 Ma experienced transient high-pressure metamorphism (Fig. 6C). The northern part of the Isukasia terrane is devoid of low Th/U metamorphic zircon overgrowths formed at ~2970 Ma, indicating lower metamorphic grade at that time. This part of the Isukasia terrane is interpreted as distal from the collision between a Kapisilik Mesoarchaean juvenile arc and the edge of the terrane at ~2970 Ma (Fig. 6C).

6.2. Reworking of the ~2970 Ma collisional architecture by ~2690 Ma intra-crustal shear zones

Metamorphosed mylonites 1 and 2 that are the boundaries between the two portions of the Isukasia terrane and the northern Kapisilik terrane, contain ~2690 Ma metamorphic zircons. On the other hand, ~2690 Ma U-Pb mineral dates in the intervening areas are more sporadic. We suggest that these mylonites reflect deep portions of shear zones active at 2690 Ma (Fig. 6D). We note that all these shear zones in their present state have been strongly modified by ductile deformation (late folding and shearing under amphibolite facies). Therefore the evidence of the initial temperature at which they formed and the related kinematic indicators have been destroyed. These shear zones could represent the re-deformed original Mesoarchaean terrane boundaries, or they could be new Neoarchaean structures that excised the earlier terrane boundaries. There is not enough structural information preserved to distinguish between these two options – which actually offer variations of a single model, rather than suggest two conflicting models. Regardless of these two options, the Neoarchaean deformation telescoped the Mesoarchaean orogen, so that Isukasia terrane hinterland remote from the collision (northern Isukasia area), and juvenile arc rocks in the Kapisilik terrane are now found within 15 km of each other (Fig. 1). Post ~2690 Ma, these mylonites were folded (Fig. 1).

6.3. Mesoarchaean crustal evolution in the Nuuk region

Assembly of the Isukasia terrane with younger crust occurred in the Mesoarchaean (Hanmer et al., 2002; Friend and Nutman, 2005). However, as pointed out by Friend and Nutman (2005), this finding does to invalidate interpretations of Neoarchaean terrane assembly in the southern part of the Nuuk region, which is supported by a wealth of structural, metamorphic and U-Pb geochronological evidence (Friend et al., 1987, 1988, 1996; Nutman et al., 1989; Crowley, 2002; Nutman and Friend, 2007; Dziggel et al., 2014). Instead, we propose that following on from the assembly of the Isukasia and Kapisilik terranes by 2970 Ma, the resulting collisional orogen was modified by a series of Neoarchaean tectonic events. The first was the development of several shear zones with some component of reverse movement (mylonites 1 to 3; Fig. 1). We regard the formation of these mylonites as probably a far field effect related to the ~2700 Ma assembly of the Færingehavn, Tre Brødre and Tasiusarsuaq terranes in the southern part of the Nuuk region (Friend et al., 1996; Crowley, 2002; Nutman and Friend, 2007; Dziggel et al., 2014). Thus crustal shortening at ~2700 Ma generated a series of thrusts, subsequently steepened by folding, and represented by folded mylonites 1-3 (Fig. 1);

mylonite 3 brought an allochthonous terrane affected by 2720-2700 Ma high grade metamorphism and granite intrusion to overlie the northern Kapisilik terrane *not* affected by these events; between mylonites 2 and 1 are rocks affected by ~2970 Ma metamorphism and granite intrusion, whereas the Isukasia terrane north of mylonite 1 was not affected (Fig. 6D). In the late Neoarchaean, the ~2970 Ma collisional architecture was further disrupted, first by folding to form a series of non-cylindrical antiforms and synforms, and then in the west by further dislocation over steep shear zones which we correlate with the ~2540 Ma (Nutman et al., 2010) Ivinguit fault farther south in the Nuuk region.

In the Nuuk region there was an initial collision by 2970 Ma of a ~3000 Ma juvenile arc (in Kapisilik terrane) with the Eoarchaean rocks of the Isukasia terrane, and then, approximately 200 million years later, they were juxtaposed with 2920-2800 Ma arc-related rocks in the Tasiusarsuaq and Tre Brødre terranes in a second collisional orogeny with transient high pressure metamorphism (Nutman et al., 1989, Friend et al., 1996; Crowley, 2002; Nutman and Friend, 2007; Dziggel et al., 2014). The complexity of the Archaean events documented in the Isukasia and Kapisilik terranes resembles that found in younger orogens, up to the Cenozoic. The resemblance is particularly striking when examples are considered for the initial collision between an arc and a continental mass followed by a second collision related to ocean closure.

An analogy to the Archaean superimposed orogenic events described in this paper is given by ocean closure in the Appalachians, where at ~420 Ma there was an initial Taconic orogeny caused by the arrival of the juvenile Taconic arc complex against the eastern passive margin of North America (e.g., Hatcher, 2010 and references therein). This can be taken as an analogy of the emplacement of the juvenile Kapisilik terrane against the Eoarchaean Isukasia terrane. Subsequently in the Appalachian analogy, exotic blocks of Avalonia were added to the North American margin at ~370 Ma in the Acadian orogeny, followed by final ocean closure by the arrival of Africa, resulting in the 325-260 Ma Alleghenian orogeny (Hatcher, 2010). The latter orogenies partitioned and disrupted the tectonic architecture of the initial juxtaposition of the juvenile Taconic arc complex against North America (Hatcher, 2010), and can be likened to the ~2690 Ma shearing events that affected the Mesoarchaean relationship between the Isukasia and Kapisilik terranes.

7. Conclusions

(1) Neoarchaean mylonites separate the northern and southern parts of the Isukasia terrane and the northern Kapisilik terrane into domains with different pre-Neoarchaean metamorphic histories.

(2) These mylonites are interpreted to have dislocated an earlier collisional orogenic relationship (~2970 Ma) between the Eoarchaean (continental) Isukasia terrane and the Mesoarchaean (juvenile arc) Kapisilik terrane.

(3) At ~2970 Ma crustal thickening resulted in transient high-pressure metamorphism in the southern part of the Isukasia terrane. In that part of the Isukasia terrane buried under the Kapisilik terrane arc, partial melting formed granites and granodiorites with negative ε_{Hf} (2970) magmatic zircon, that rose to higher crustal levels and were emplaced into the allochthonous juvenile arc rocks.

(4) The sequence of Meso- Neoarchaean events established for the Isukasia terrane and the northern parts of the Kapisilik terrane resemble those seen in Phanerozoic orogenies, where

an island arc collides with an older continental mass and the resulting architecture is disturbed by later tectonic events.

Acknowledgments

Between 2003 and 2005 support to APN and CRLF was via Australian Research Council grant DP0342798. The Korean Basic Research Institute supported dating of sample G05/26. There was logistical support and help in the field over many years from Ole Christiansen of Nunaminerals A/S. We thank Ali Polat and an anonymous reviewer for constructive comments.

References

Allaart, J.H., 1982. Geological map of Greenland 1:500,000, sheet 2, Frederikshaab Isblink – Søndre Stromfjord. Grønlands Geologiske Undersøgelse, Copenhagen.

Baadsgaard, H., 1976. Further U-Pb dates on zircons from the early Precambrian rocks of the Godthaabsfjord area, West Greenland. Earth and Planetary Science Letters 33, 261-267.

Baadsgaard, H, McGregor, V.R., 1981. The U-Th-Pb systematics of zircons from the type Nûk gneisses, Godthåbsfjord, West Greenland. Geochimica et Cosmochimica Acta 45, 1099-1109.

Black, L.P., Kamo, S.L., Allen, C.M., Aleinikoff, J.M., Davis, D.W., Korsch, R.J., Foudoulis, C., 2003. TEMORA 1: A new zircon standard for Phanerozoic U-Pb geochronology. Chemical Geology 200, 155–170.

Bouvier A., Vervoort J.D., Patchett J., 2008. The Lu–Hf and Sm–Nd isotopic composition of CHUR: constraints from unequilibrated chondrites and implications for the bulk composition of the terrestrial planets. Earth and Planetary Sciences Letters 280, 285–295, doi:10.1016/j.epsl.2008.06.010.

Bridgwater, D., McGregor, V.R., 1974. Field work on the very early Precambrian rocks of the Isua area, southern West Greenland. Rapport Grønlands Geologiske Undersøgelse 65, 49-54.

Chadwick, B., 1985. Contrasting styles of tectonism and magmatism in the late Archaean crustal evolution of the northeastern part of the Ivisârtoq region, inner Godthåbsfjord, southern West Greenland. Precambrian Research, 27, 215–238.

Chadwick, B., 1990. The stratigraphy of a sheet of supracrustal rocks within highgrade orthogneisses and its bearing on Late Archaean structure in southern West Greenland. Journal of the Geological Society of London 147, 639–652.

Chadwick, B., Coe, K., 1988. 1:100 000 Ivisârtoq (64V.2 Nord). Geological Survey of Denmark and Greenland, Copenhagen.

Chu, M-F., Chun, S-L., Song, B., Liu, D-Y., O'Reilly, S.Y., Pearson, N.J., Ji, J., Wen, D-J., 2002. Zircon U-Pb and Hf isotope constraints on the Mesozoic tectonics and crustal evolution of southern Tibet. Geology 34, 745-748, doi: 10.1130/G22725.1.

Coney, P.J., Jones, D.L., Monger, J.W.H., 1980. Cordilleran suspect terranes. Nature 288, 329-333.

Crowley, J.L. 2002. Testing the model of late Archean terrane accretion in southern West Greenland: a comparison of timing of geological events across the Qarliit Nunaat fault, Buksefjorden region. Precambrian Research 116, 57-79.

Crowley, J.L., 2003. U-Pb geochronology of 3810-3630 Ma granitoid rocks south of the Isua greenstone belt, southern West Greenland. Precambrian Research 126, 235-257.

Crowley, J.L., Myers, J.S., Dunning, G.R., 2002. Timing and nature of multiple 3700-3600 Ma tectonic events in intrusive rocks north of the Isua greenstone belt, southern West Greenland. Geological Society of America Bulletin 114, 1311-1325.

Dziggel, A., Diener, J.F.A., Kolb, J., Kokfelt, T.F., 2014. Metamorphic record of accretionary processes during the Neoarchaean: The Nuuk region, southern West Greenland. Precambrian Research 242, 22-38.

Friend, C.R.L., Kinny, P.D., 2001. A reappraisal of the Lewisian Gneiss Complex: geochronological evidence for its tectonic assembly from disparate terranes in the Proterozoic. Contributions to Mineralogy and Petrology 142, 198-218.

Friend, C.R.L., Nutman, A.P., 2005. New pieces to the Archaean terrane jigsaw puzzle in the Nuuk region, southern West Greenland: Steps in transforming a simple insight into a complex regional tectonothermal model. Journal of the Geological Society, London 162, 147-163.

Friend, C.R.L., Nutman, A.P., McGregor, V.R., 1987. Late Archaean tectonics in the Færingehavn - Tre Brødre area, Buksefjorden, southern West Greenland. Journal of the Geological Society of London 144, 369-376.

Friend, C.R.L., Nutman, A.P., McGregor, V.R., 1988. Late Archaean terrane accretion in the Godthåb region, southern West Greenland. Nature 335, 535-538.

Friend, C.R.L., Nutman, A.P., Baadsgaard, H., McGregor, V.R., Kinny, P.D. 1996. Timing of late Archaean terrane assembly, granite emplacement and metamorphism in the Nuuk region, southern West Greenland. Earth and Planetary Science Letters 142, 353-366.

Garde, A.A., 2007. A mid-Archaean island arc complex in the eastern Akia terrane, Godthåbsfjord, southern West Greenland. Journal of the Geological Society, London, 164, 565–579.

Garde, A.A., Friend, C.R.L., Marker, M., Nutman, A.P., 2001. Rapid maturation and stabilisation of middle Archaean continental crust: the Akia terrane, southern West Greenland. Bulletin of the Geological Society of Denmark 47, 1-27.

Hall, R.P., Friend, C.R.L., 1979. Structural evolution of the Archaean rocks in Ivisârtoq and the neighbouring inner Godthåbsfjord region, southern West Greenland. Geology 7, 311-315.

Hall, R.P., Friend, C.R.L., 1983. Intrusive relationships between young and old Archaean gneisses: evidence from Ivisârtoq, southern West Greenland. Geological Journal 18, 77-91.

Hanmer, S., Hamilton, M.A., Crowley, J.L., 2002. Geochronological constraints on Paleoarchean thrust nappe and Neoarchean accretionary tectonics in southern West Greenland. Tectonophysics 350, 255-271.

Hatcher, R.D., 2010. The Appalachian orogen: A brief summary. Geological Society of America Memoirs 206, 1-19.

Hiess, J., Bennett, V.C., Nutman, A.P., Williams, I.S., 2009. In situ U-Pb, O and Hf isotopic compositions of zircon from Eoarchaean tonalite and felsic volcanic rocks, Itsaq Gneiss Complex, southern West Greenland: New constraints on the source materials for the early crust. Geochimica et Cosmochimica Acta 73, 4489-4516.

Jenner, F.E., 2006. Geochemistry and petrochemistry of Archaean mafic and ultramafiuc rocks, southern West Greenland. Australian National University PhD Thesis, Canberra, pp. 275.

Kalsbeek, F., Garde, A.A., 1989. Descriptive text to 1:500,000 sheet 2, Frederikshaab Isblink – Søndre Stromfjord. 36 pp. Grønlands Geologiske Undersøgelse, Copenhagen.

Ludwig, K.R., 2003. Isoplot 3.0: A geochronological toolkit for Microsoft Excel, Berkeley Geochronological Center Special Publication 4, 70 pp., Berkeley Geochronological Center, Berkeley, California.

McGregor, V.R., Friend, C.R.L., Nutman, A.P., 1991. The late Archaean mobile belt through Godthåbsfjord, southern West Greenland: a continent-continent collision zone? Bulletin of the Geological Society of Denmark 39, 179-197.

Nielsen, S.G., Baker, J.A., Krogstad, E.J., 2002. Petrogenesis of an early Archean (3.4 Ga) norite dyke, Isua West Greenland: evidence for early Archean crustal recycling. Precambrian Research 118, 133-148.

Nutman, A.P., 1984. Early Archaean crustal evolution of the Isukasia area, southern West Greenland. In: Precambrian Tectonics Illustrated (A. Kröner & R. Grieling editors), E. Schweizerbart'sche Verlagsbuchhandlung, Stuttgart.

Nutman, A.P., 1986. The geology of the Isukasia area southern West Greenland. Bulletin Grønlands Geologiske Undersøgelse 154, 80 pp.

Nutman, A.P., Collerson, K.D., 1991. Very early Archean crustal-accretion complexes preserved in the North Atlantic Craton. Geology 19, 791-795.

Nutman, A.P., Friend, C.R.L., 2007. Terranes with ca. 2715 and 2650 Ma high-pressure metamorphisms juxtaposed in the Nuuk region, southern West Greenland: Complexities of Neoarchaean collisional orogeny. Precambrian Research 155, 159-203.

Nutman, A.P., Friend, C.R.L., 2009. New 1:20,000 scale geological maps, synthesis and history of investigation of the Isua supracrustal belt and adjacent orthogneisses, southern West Greenland: A glimpse of Eoarchaean crust formation and orogeny. Precambrian Research, 172, 189-211.

Nutman, A.P., Bennett, V.C., Friend, C.R.L., Rosing, M.T., 1997. ~3710 and ≥3790 Ma volcanic sequences in the Isua (Greenland) supracrustal belt; structural and Nd isotope implications. Chemical Geology 141, 271-287.

Nutman, A.P., Bennett, V.C., Friend, C.R.L., Hidaka, H., Yi, K., Lee, S.R., Kamiichi, T., 2013. Episodic 3920-3660 Ma juvenile crust formation and 3660-3600 Ma recycling in the Itsaq Gneiss Complex of southern West Greenland. American Journal of Science 313, 877-911. DOI: 10.2475/09.2013.00

Nutman, A.P., Friend, C.R.L., Baadsgaard, H., McGregor, V.R., 1989. Evolution and assembly of Archean gneiss terranes in the Godthåbsfjord region, southern West Greenland: Structural, metamorphic, and isotopic evidence. Tectonics 8, 573-589.

Nutman, A.P., Friend, C.R.L., Bennett, V.C., McGregor, V.R., 2000. The early Archaean Itsaq Gneiss Complex of southern West Greenland: The importance of field observations in interpreting dates and isotopic data constraining early terrestrial evolution. Geochimica et Cosmochimica Acta 64, 3035-3060.

Nutman, A.P., Friend, C.R.L., Bennett, V.C., 2002. Evidence for 3650-3600 Ma assembly of the northern end of the Itsaq Gneiss Complex, Greenland: Implication for early Archean tectonics. Tectonics 21, article 5

Nutman, A.P., Friend, C.R.L., Barker, S.L.L., McGregor, V.R., 2004a. Inventory and assessment of Palaeoarchaean gneiss terrains and detrital zircons in southern West Greenland. Precambrian Research 135, 281-314.

Nutman, A.P., Friend, C.R.L., Bennett, V.C., 2004b. Dating of the Ameralik dyke swarms of the Nuuk district, southern West Greenland: Mafic intrusion events starting from c. 3510 Ma. Journal of the Geological Society, London 161, 421-430.

Nutman, A.P., Friend, C.R.L., Horie, H., Hidaka, H., 2007. Construction of pre-3600 Ma crust at convergent plate boundaries, exemplified by the Itsaq Gneiss Complex of southern West Greenland. *In:* van Kranendonk, M.J., Smithies, R.H., & Bennett, V.C. (eds) *Earth's Oldest Rocks*. Elsevier, pp.187-218.

Nutman, A.P., Friend, C.R.L., Hiess, J., 2010. Setting of the ~2560 Ma Qôrqut granite complex in the Archaean crustal evolution of southern West Greenland. American Journal of Science 310, 1081-1114.

Nutman, A.P., McGregor, V.R., Friend, C.R.L., Bennett, V.C., Kinny, P.D., 1996. The Itsaq Gneiss Complex of southern West Greenland; the world's most extensive record of early crustal evolution (3900-3600 Ma). Precambrian Research 78, 1-39.

Næraa, T., Scherstén, A., Rosing, M.T., Kemp, A.I.S., Hoffmann, J.E., Kokfelt, T.F., Whitehouse, M.J., 2012. Hafnium isotope evidence for a transition in the dynamics of continental growth 3.2 Gyr ago. Nature 485, 627-630.

Ordóñez-Calderón, J.C., Polat, A., Fryer, B., Appel, P.W.U., van Gool, J.A.M., Dilek, Y., Gagnon, J.E., 2009. Geochemistry and geodynamic origin of Mesoarchean oceanic crust in the Ujarassuit and Ivisaartoq greenstone belts, SW Greenland. Lithos 113, 133.

Paces, J.B., Miller, J.D.Jr., 1993. Precise U-Pb ages of Duluth Complex and related mafic intrusions, northeastern Minnesota: Geochronological insights to physical, petrogenetic, paleomagnetic and tectonomagmatic processes associated with the 1.1 Ga midcontinent rift system. Journal of Geophysical Research 98, 13997-14013.

Park, J.F.W., 1987. Fault systems in the inner Godthåbsfjord region of the Archaean block, southern West Greenland. PhD thesis, University of Exeter.

Patchett P. J., Kouvo O., Hedge C. E., Tatsumoto M., 1981. Evolution of continental crust and mantle heterogeneity: evidence from Hf isotopes. Contributions to Mineralogy and Petrology 78, 279–297.

Polat, A., Appel, P.W.U., Frei, R., Pan, W.M., Dilek, Y., Ordonez-Calderon, J.C., Fryer, B., Hollis, J.A., Raith, J.G., 2007. Field and geochemical characteristics of the Mesoarchean (~3075 Ma) Ivisaartoq greenstone belt, southern West Greenland: Evidence for seafloor hydrothermal alteration in supra-subduction oceanic crust. Gondwana Research 11, 69-91.

Polat, A., Frei, R., Appel, P.W.U., Dilek, Y., Freyer, B., Ordonez-Calderon, J.C., Yang, Z., 2008. The origin and compositions of Mesoarchean oceanic crust: Evidence from the 3075 Ma Ivisaartoq greenstone belt, SW Greenland. Lithos 100, 293-321.

Rasmussen, T.M., Thorning, L., 1999. Airborne geophysical survey in Greenland in 1998. Geology of Greenland Survey Bulletin 183, 34-38, Geological Survey of Denmark and Greenland, Copenhagen.

Russell, W.A., Papanastassiou D.A., Tombrello, T.A., 1978. Ca isotope fractionation on the Earth and other solar system material. Geochimica et Cosmochimica Acta 42, 1075–1090.

Scherer, E., Münker C., Mezger, K., 2001. Calibration of the lutetium–hafnium clock. Science 293, 683–687.

Söderlund, U., Patchett P.J., Vervoort J.D., Isachsen, C.E., 2004. The ^{176}Lu decay constant determined by Lu–Hf and U–Pb isotope systematics of Precambrian mafic intrusions. Earth and Planetary Science Letters 219, 311–324.

Szilas, K., Van Hinsberg, V.J., Kisters, A.F.M., Hoffmann, J.E., Windley, B.F., Kokfelt, T.F., Schersten, A., Frei, R., Rosing, M.T., Münker, C., 2013. Remnants of arc-related Mesoarchaean oceanic crust in the Tartoq Group of SW Greenland. Gondwana Research 23, 436-451.

Woodhead, J., Hergt, J., 2005. A preliminary appraisal of seven natural zircon reference materials for in situ Hf isotope determination. Geostandards and Geoanalytical Research, 29, 183–195.

Woodhead, J., Hergt, J., Shelley, M., Eggins, S., Kemp R., 2004. Zircon Hf-isotope analysis with an excimer laser, depth profiling, ablation of complex geometries, and concomitant age estimation. Chemical Geology 209, 121–135.

Vervoort, J.D., Patchett, P.J., Söderlund, U., Baker, M., 2004. Isotopic composition of Yb and the determination of Lu concentrations and Lu/Hf ratios by isotope dilution using MC-ICPMS. Geochemistry, Geophysics and Geosystems 5, DOI: 10.1029/2004GC000721.

Zeck, H. Williams, I.S., 2001. Hercynian metamorphism in nappe core complexes of the Alpine Betic-Rif Belt, western Mediterranean – a SHRIMP zircon study. Journal of Petrology 42, 1373-1385.

Figure and Table Captions

Figure 1. Geological map of the Isukasia – Ivisaartoq study area, southern West Greenland. Location of samples discussed in text is indicated. * The Isua supracrustal belt has numerous dating sites (e.g., Nutman and Friend, 2009). These are not shown on this figure.

Figure 2. Summary of metamorphic ages and rocks of the Kapisilik terrane. % of dated samples refers to proportion of samples within the terrane whose zircons show metamorphic overgrowths.

Figure 3. (A) ~3500 Ma Ameralik dyke (ad) strongly discordant to agmatitic structures in host ~3800 Ma tonalites of the Itsaq Gneiss Complex, ~10 km south of the Isua supracrustal belt. Although the dyke is little-deformed, they have been recrystallised during superimposed Neoarchaean amphibolite facies metamorphism. (B) Ameralik dykes (ad) in the domain between mylonite-1 and mylonite-2. The dykes are highly attenuated by ductile deformation to be concordant with layering in their host gneisses and have been disrupted disrupted by pegmatite (peg). (C) Plane polarised light photomicrograph of sample G12/141 (64°58.60'N 49°56.70'W) with high-pressure granulite assemblage (gnt = garnet, cpx = clinopyroxene, plag+qtz = plagioclase + quartz, hbl = hornblende, epi = epidote-rich domains). The original garnet + clinopyroxene + plagioclase + quartz assemblage has been strongly retrogressed, giving rise to epidote-rich domains in plagioclase and hornblende rims on garnet and clinopyroxene. (D) Domain between mylonites 2 and 3, ~10 km southwest of the Isua supracrustal belt. Migmatitic gneisses containing vestiges of Ameralik dykes (ad) as tabular bodies (foreground) and as schlieren in neosome

(background). This indicates post-Ameralik dyke migmatisation/reworking of Itsaq Gneiss Complex rocks.

Figure 4. Tera-Wasserburg (^{207}Pb/^{206}Pb – ^{238}U/^{206}Pb) plots of zircon data (shown with 2 sigma analytical errors). (A) G05/26 felsic patch in youngest generation of Ameralik dykes; (B) G91/82 mylonite-1; (C) G12/165 garnet mica schist; (D) G93/88 mylonite-2; (E) G04/05 granite; (F) G03/75 migmatite.

Figure 5. Plot or zircon U-Pb age versus ε_{Hf}-tzirc. See text for explanation and discussion.

Figure 6. Cartoon sections illustrating crustal evolution in the Isua – Ujaragssuit – Ivisaartoq region. (A) 3075 juvenile arc; (B) Continued development of juvenile arc complex(es) in the Kapisilik terrane and convergence with the Isukasia terrane; (C) 2970 Ma collision, crustal thickening and crustal melting; (D) 2690 Ma partitioning, proposed as a far-field effect of terrane assembly on the present outer coast region to the southwest.

Table 1. Summary SHRIMP zircon U-Th-Pb data

Table 2. Summary LAICPMS zircon Lu-Hf data

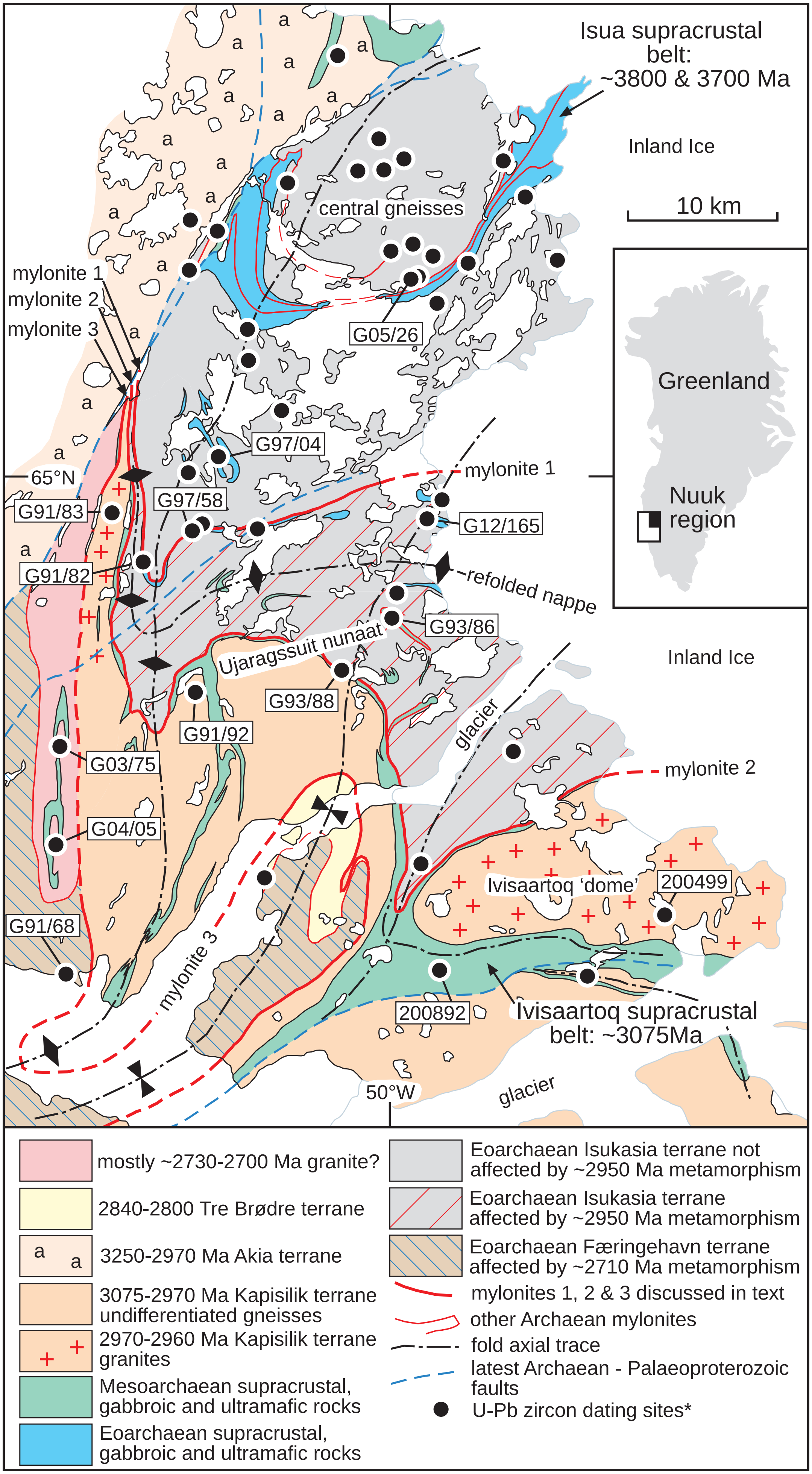

Isua supracrustal belt: ~3800 & 3700 Ma
Inland Ice
10 km
central gneisses
mylonite 1
mylonite 2
mylonite 3
G05/26
G97/04
G97/58
65°N
G91/83
G91/82
G12/165
refolded nappe
G93/86
Ujaragssuit nunaat
G93/88
G91/92
glacier
G03/75
G04/05
G91/68
Ivisaartoq 'dome'
200499
200892
Ivisaartoq supracrustal belt: ~3075Ma
50°W
glacier
Greenland
Nuuk region
mostly ~2730-2700 Ma granite?
2840-2800 Tre Brødre terrane
3250-2970 Ma Akia terrane
3075-2970 Ma Kapisilik terrane undifferentiated gneisses
2970-2960 Ma Kapisilik terrane granites
Mesoarchaean supracrustal, gabbroic and ultramafic rocks
Eoarchaean supracrustal, gabbroic and ultramafic rocks
Eoarchaean Isukasia terrane not affected by ~2950 Ma metamorphism
Eoarchaean Isukasia terrane affected by ~2950 Ma metamorphism
Eoarchaean Færingehavn terrane affected by ~2710 Ma metamorphism
mylonites 1, 2 & 3 discussed in text
other Archaean mylonites
fold axial trace
latest Archaean - Palaeoproterozoic faults
U-Pb zircon dating sites*

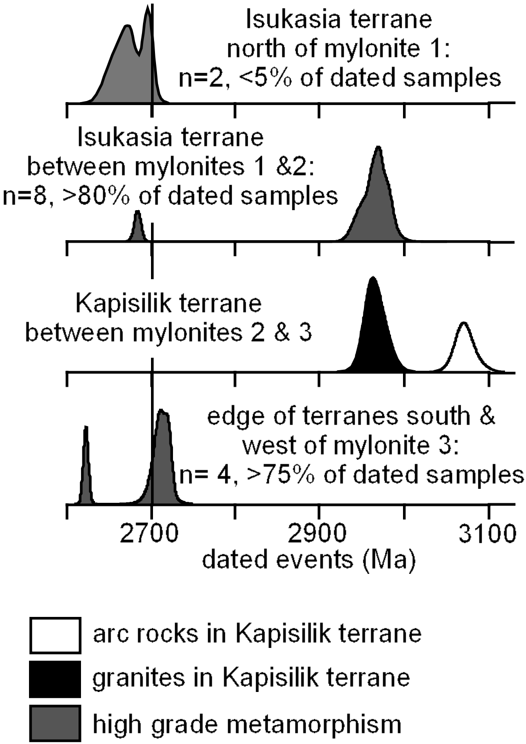
Isukasia terrane
north of mylonite 1:
n=2, <5% of dated samples
Isukasia terrane
between mylonites 1 &2:
n=8, >80% of dated samples
Kapisilik terrane
between mylonites 2 & 3
edge of terranes south &
west of mylonite 3:
n= 4, >75% of dated samples
2700
2900
3100
dated events (Ma)
arc rocks in Kapisilik terrane
granites in Kapisilik terrane
high grade metamorphism

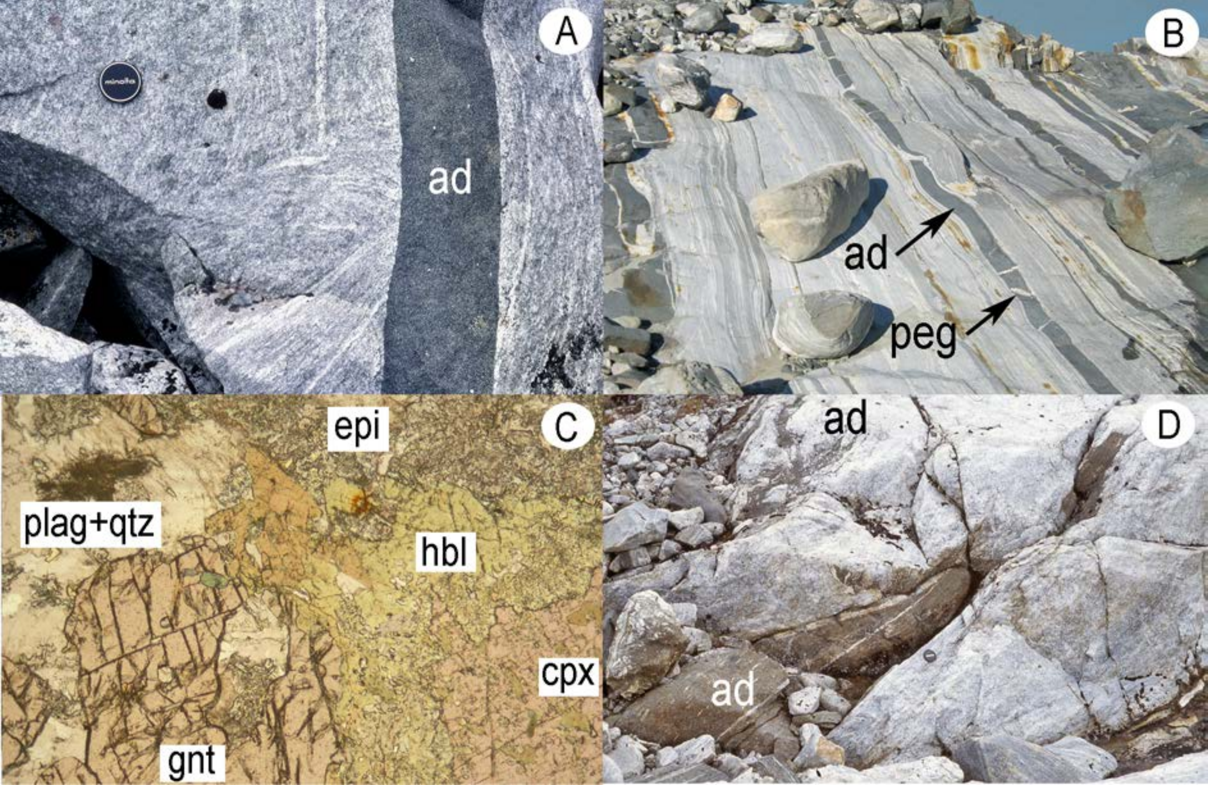
A
ad
B
ad
peg
C
epi
plag+qtz
hbl
cpx
gnt
D
ad
ad

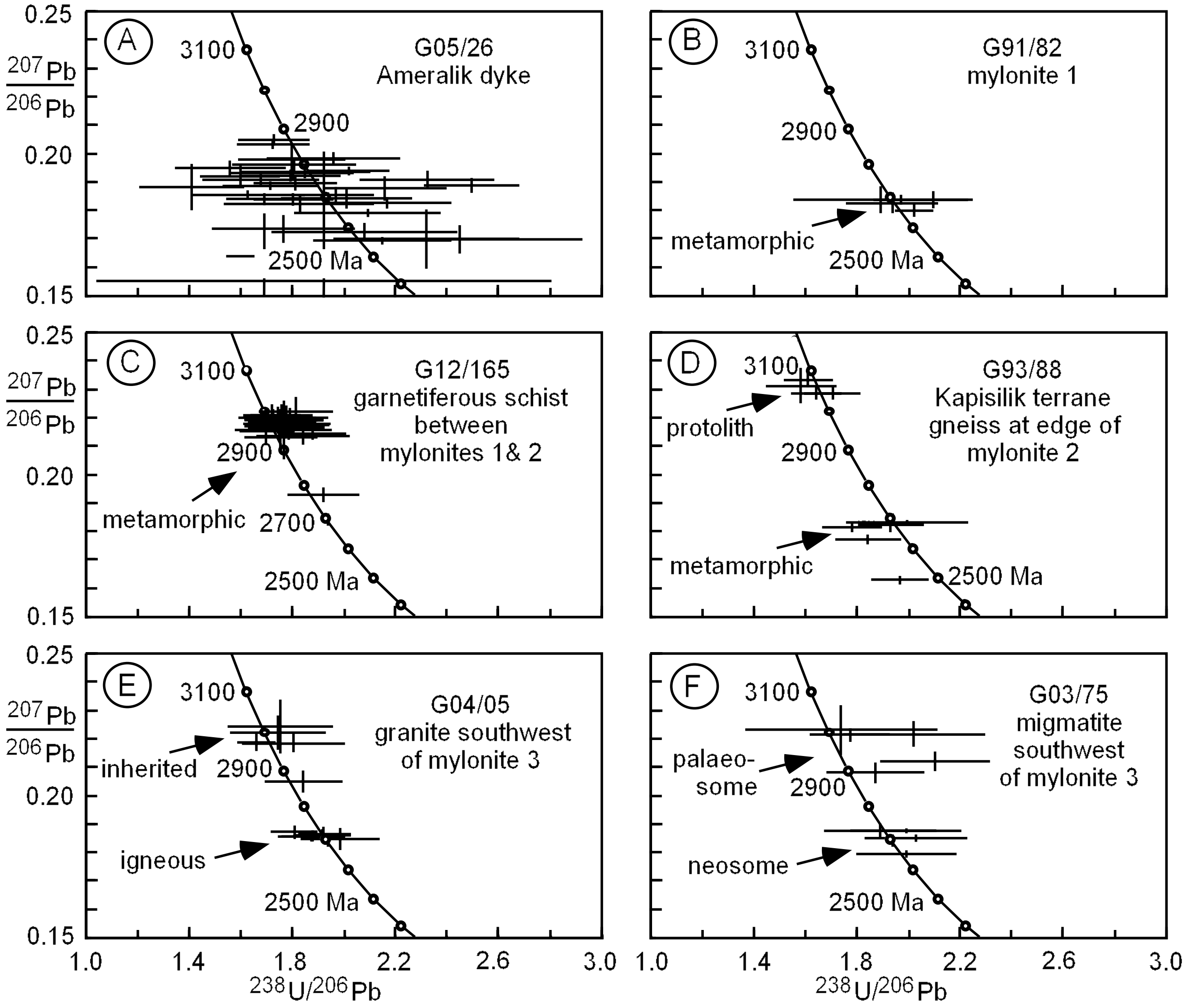

0.25
0.20
0.15
$^{207}Pb/^{206}Pb$
A
G05/26
Ameralik dyke
3100
2900
2500 Ma
B
G91/82
mylonite 1
3100
2900
metamorphic
2500 Ma
C
G12/165
garnetiferous schist
between
mylonites 1& 2
3100
2900
metamorphic
2700
2500 Ma
D
G93/88
Kapisilik terrane
gneiss at edge of
mylonite 2
3100
protolith
2900
metamorphic
2500 Ma
E
G04/05
granite southwest
of mylonite 3
3100
inherited
2900
igneous
2500 Ma
F
G03/75
migmatite
southwest
of mylonite 3
3100
palaeo-
some
2900
neosome
2500 Ma
1.0
1.4
1.8
2.2
2.6
3.0
$^{238}U/^{206}Pb$

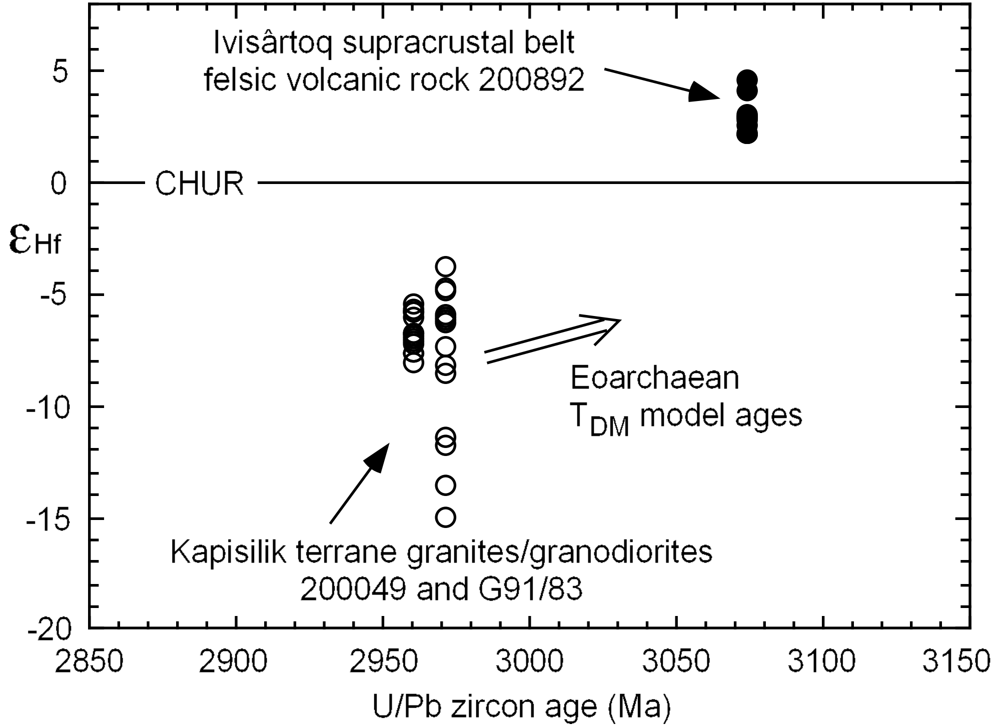
Ivisârtoq supracrustal belt
felsic volcanic rock 200892
CHUR
Eoarchaean
T_{DM} model ages
Kapisilik terrane granites/granodiorites
200049 and G91/83
ε_{Hf}
U/Pb zircon age (Ma)
5
0
-5
-10
-15
-20
2850
2900
2950
3000
3050
3100
3150

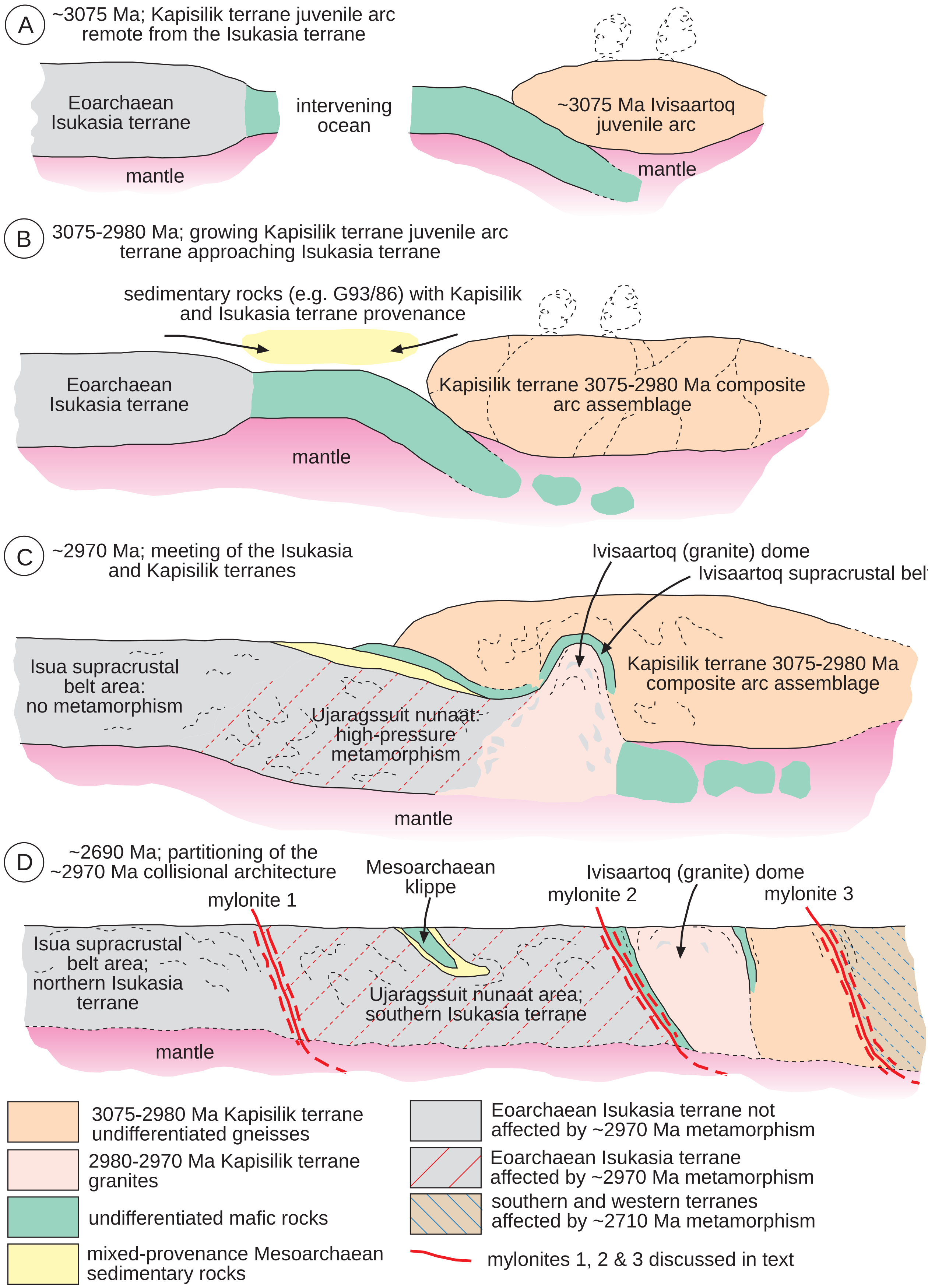

A
~3075 Ma; Kapisilik terrane juvenile arc remote from the Isukasia terrane
Eoarchaean Isukasia terrane
intervening ocean
~3075 Ma Ivisaartoq juvenile arc
mantle
mantle
B
3075-2980 Ma; growing Kapisilik terrane juvenile arc terrane approaching Isukasia terrane
sedimentary rocks (e.g. G93/86) with Kapisilik and Isukasia terrane provenance
Eoarchaean Isukasia terrane
Kapisilik terrane 3075-2980 Ma composite arc assemblage
mantle
C
~2970 Ma; meeting of the Isukasia and Kapisilik terranes
Ivisaartoq (granite) dome
Ivisaartoq supracrustal belt
Isua supracrustal belt area: no metamorphism
Ujaragssuit nunaat: high-pressure metamorphism
Kapisilik terrane 3075-2980 Ma composite arc assemblage
mantle
D
~2690 Ma; partitioning of the ~2970 Ma collisional architecture
Mesoarchaean klippe
Ivisaartoq (granite) dome
mylonite 1
mylonite 2
mylonite 3
Isua supracrustal belt area; northern Isukasia terrane
Ujaragssuit nunaat area; southern Isukasia terrane
mantle
3075-2980 Ma Kapisilik terrane undifferentiated gneisses
2980-2970 Ma Kapisilik terrane granites
undifferentiated mafic rocks
mixed-provenance Mesoarchaean sedimentary rocks
Eoarchaean Isukasia terrane not affected by ~2970 Ma metamorphism
Eoarchaean Isukasia terrane affected by ~2970 Ma metamorphism
southern and western terranes affected by ~2710 Ma metamorphism
mylonites 1, 2 & 3 discussed in text

Table 1: SHRIMP U/Pb zircon analyses

labels	U ppm	Th ppm	Th/U	comm. 206Pb%	238U / 206/Pb ratio	207Pb / 206Pb ratio	207 / 206 date (Ma)	%conc
G05/26 felsic patch in Ameralik dyke								
B1.1	9067	8439	####	0.036	1.767 ± 0.137	0.1739 ± 0.0022	2595 ± 22	111
B2.1	1614	920	####	0.043	2.322 ± 0.179	0.1703 ± 0.0050	2561 ± 50	90
B3.1	6331	6909	####	0.056	1.923 ± 0.440	0.1554 ± 0.0227	2406 ± 273	112
B4.1	3648	2105	####	0.038	1.717 ± 0.091	0.1892 ± 0.0005	2735 ± 5	108
B5.1	5228	6933	####	0.022	2.161 ± 0.118	0.1883 ± 0.0020	2727 ± 17	90
B6.1	2375	1707	####	0.039	1.800 ± 0.102	0.1986 ± 0.0027	2814 ± 22	101
B7.1	2831	1032	####	0.038	1.598 ± 0.075	0.1926 ± 0.0018	2765 ± 15	113
B8.1	3308	4284	####	0.018	1.677 ± 0.110	0.1914 ± 0.0009	2754 ± 8	109
B9.1	1508	1496	####	0.034	1.960 ± 0.127	0.1990 ± 0.0009	2818 ± 8	94
B10.1	4935	4658	####	0.046	1.828 ± 0.144	0.1827 ± 0.0014	2678 ± 13	105
B11.1	4488	8479	####	6.200	2.150 ± 0.132	0.1697 ± 0.0005	2554 ± 5	96
B12.1	1562	118	####	0.019	1.970 ± 0.071	0.1858 ± 0.0013	2706 ± 11	98
B12.2	7883	9190	####	0.175	7.737 ± 0.564	0.1421 ± 0.0011	2253 ± 14	35
B13.1	875	88	####	0.174	2.451 ± 0.238	0.1701 ± 0.0023	2559 ± 23	86
B13.2	2564	947	####	0.317	1.805 ± 0.075	0.1844 ± 0.0009	2692 ± 8	106
B14.1	4916	4825	####	0.050	2.167 ± 0.122	0.1831 ± 0.0008	2682 ± 7	91
B14.2	5366	5243	####	0.012	1.795 ± 0.095	0.1928 ± 0.0008	2766 ± 7	103
W1.1	3518	2260	####	0.023	2.011 ± 0.124	0.1847 ± 0.0016	2696 ± 14	97
W2.1	5751	6567	####	0.044	1.690 ± 0.070	0.1844 ± 0.0009	2693 ± 8	111
W3.1	2046	900	####	0.098	1.802 ± 0.117	0.1937 ± 0.0008	2774 ± 7	103
W4.1	5656	10211	####	0.041	1.850 ± 0.124	0.1942 ± 0.0009	2778 ± 8	100
W4.2	5145	4953	####	0.047	1.558 ± 0.105	0.1955 ± 0.0012	2789 ± 10	115
W5.1	2382	3623	####	0.001	1.730 ± 0.068	0.2055 ± 0.0008	2870 ± 6	103
W5.2	4021	3133	####	0.017	1.808 ± 0.117	0.1967 ± 0.0010	2799 ± 9	101
W6.1	3768	2970	####	0.031	1.812 ± 0.079	0.1901 ± 0.0011	2743 ± 10	103
W7.1	3363	2210	####	0.025	1.629 ± 0.108	0.1858 ± 0.0006	2706 ± 5	114
W8.1	6695	11081	####	0.006	1.695 ± 0.073	0.1640 ± 0.0075	2498 ± 79	120
W9.1	5538	14740	####	0.008	1.409 ± 0.099	0.1887 ± 0.0039	2731 ± 35	127
W9.2	5334	7530	####	0.002	2.093 ± 0.141	0.1796 ± 0.0005	2649 ± 4	95
W10.1	3254	3145	####	0.056	2.325 ± 0.129	0.1914 ± 0.0014	2754 ± 12	84
W11.1	5196	4861	####	0.015	2.081 ± 0.178	0.1728 ± 0.0014	2585 ± 13	98
W12.1	3288	3655	####	0.077	2.020 ± 0.077	0.1945 ± 0.0006	2781 ± 5	93
W13.1	4105	3124	####	0.006	1.726 ± 0.069	0.2038 ± 0.0006	2857 ± 5	103
W14.1	1576	994	####	0.040	2.498 ± 0.091	0.1893 ± 0.0011	2736 ± 9	79
G91/82 meta-mylonite								
1.1	1203	21	####	0.058	2.098 ± 0.073	0.1839 ± 0.0013	2688 ± 12	94
2.1	234	18	####	0.434	1.890 ± 0.167	0.1838 ± 0.0022	2688 ± 20	102
3.1	723	8	####	0.051	1.935 ± 0.087	0.1828 ± 0.0016	2679 ± 14	100
4.1	1940	42	####	0.034	2.020 ± 0.035	0.1801 ± 0.0009	2653 ± 8	98
5.1	549	5	####	0.062	1.968 ± 0.050	0.1839 ± 0.0006	2689 ± 6	99
G12/165 garnetiferous schist								
1.1	170	39	####	0.027	1.767 ± 0.059	0.2188 ± 0.0017	2972 ± 13	97
2.1	118	37	####	0.004	1.785 ± 0.069	0.2164 ± 0.0020	2954 ± 15	97
3.1	90	42	####	0.062	1.769 ± 0.069	0.2167 ± 0.0019	2957 ± 14	98
4.1	222	83	####	0.024	1.876 ± 0.064	0.2144 ± 0.0009	2939 ± 7	94
5.1	116	35	####	0.047	1.744 ± 0.058	0.2179 ± 0.0015	2966 ± 11	99
6.1	471	179	####	0.008	1.729 ± 0.056	0.2191 ± 0.0009	2974 ± 7	99
7.1	144	54	####	0.014	1.725 ± 0.053	0.2195 ± 0.0015	2977 ± 11	99
8.1	137	42	####	0.031	1.756 ± 0.057	0.2207 ± 0.0017	2986 ± 13	97
9.1	89	31	####	0.015	1.753 ± 0.069	0.2130 ± 0.0018	2928 ± 14	99
10.1	93	29	####	0.013	1.777 ± 0.058	0.2189 ± 0.0012	2973 ± 9	97
11.1	85	23	####	<0.001	1.790 ± 0.062	0.2193 ± 0.0019	2975 ± 14	96
12.1	249	53	####	0.020	1.752 ± 0.052	0.2170 ± 0.0013	2958 ± 9	98
13.1	152	53	####	0.032	1.920 ± 0.068	0.1929 ± 0.0010	2767 ± 9	98
14.1	157	37	####	0.010	1.752 ± 0.059	0.2191 ± 0.0010	2974 ± 7	98
15.1	84	31	####	<0.001	1.741 ± 0.073	0.2199 ± 0.0017	2980 ± 13	98
16.1	191	33	####	0.032	1.745 ± 0.057	0.2188 ± 0.0019	2972 ± 14	98
17.1	118	29	####	0.012	1.720 ± 0.054	0.2208 ± 0.0016	2986 ± 12	99
18.1	352	76	####	0.065	1.777 ± 0.083	0.2179 ± 0.0013	2965 ± 10	97
19.1	94	21	####	0.083	1.697 ± 0.050	0.2154 ± 0.0020	2947 ± 15	101
20.1	58	15	####	0.008	1.778 ± 0.077	0.2200 ± 0.0019	2980 ± 14	97
21.1	209	12	####	0.015	1.810 ± 0.053	0.2189 ± 0.0010	2973 ± 7	95
22.1	116	24	####	0.005	1.749 ± 0.065	0.2170 ± 0.0009	2959 ± 7	99
23.1	118	45	####	<0.001	1.765 ± 0.092	0.2156 ± 0.0049	2948 ± 37	98
24.1	389	215	####	0.031	1.813 ± 0.070	0.2221 ± 0.0024	2996 ± 17	95
25.1	249	100	####	0.059	1.838 ± 0.089	0.2137 ± 0.0014	2934 ± 11	95
26.1	239	76	####	0.001	1.803 ± 0.068	0.2174 ± 0.0010	2961 ± 7	96
27.1	82	20	####	<0.001	1.776 ± 0.062	0.2164 ± 0.0015	2954 ± 11	98
28.1	677	171	####	0.023	1.748 ± 0.059	0.2191 ± 0.0009	2974 ± 7	98
29.1	436	88	####	0.008	1.790 ± 0.052	0.2175 ± 0.0007	2962 ± 5	97
30.1	154	41	####	0.016	1.754 ± 0.060	0.2190 ± 0.0012	2973 ± 9	98
G04/05 granite								
1.1	111	67	####	0.028	1.741 ± 0.091	0.2220 ± 0.0027	2995 ± 20	98
1.2	1785	934	####	0.008	1.658 ± 0.034	0.2186 ± 0.0012	2970 ± 9	102
2.1	50	58	####	0.001	1.753 ± 0.100	0.2242 ± 0.0045	3011 ± 32	97
2.2	1551	94	####	0.047	1.842 ± 0.073	0.2048 ± 0.0017	2865 ± 13	98
3.1	597	276	####	0.017	1.922 ± 0.049	0.1866 ± 0.0011	2712 ± 10	100
4.1	325	144	####	0.023	1.802 ± 0.097	0.2183 ± 0.0014	2968 ± 11	96
5.1	349	103	####	0.023	1.984 ± 0.074	0.1848 ± 0.0017	2697 ± 15	98
5.2	306	85	####	0.049	1.915 ± 0.053	0.1861 ± 0.0009	2708 ± 8	100

Table 1: SHRIMP U/Pb zircon analyses

labels	U ppm	Th ppm	Th/U	comm. 206Pb%	238U / 206/Pb ratio	207Pb / 206Pb ratio	207 / 206 date (Ma)	%conc
6.1	399	47	####	0.066	1.879 ± 0.058	0.1858 ± 0.0008	2705 ± 7	102
7.1	1100	273	####	0.018	1.806 ± 0.044	0.1872 ± 0.0011	2717 ± 9	105
8.1	614	70	####	0.029	1.873 ± 0.063	0.1857 ± 0.0007	2704 ± 6	102
9.1	136	60	####	0.097	1.221 ± 0.055	0.3878 ± 0.0026	3862 ± 10	100
9.2	120	49	####	0.001	1.196 ± 0.043	0.3928 ± 0.0026	3882 ± 10	101
G03/75 migmatite								
1.1	178	166	####	0.001	1.735 ± 0.185	0.2232 ± 0.0041	3004 ± 30	98
1.2	1185	17	####	0.005	2.100 ± 0.105	0.2124 ± 0.0015	2924 ± 11	86
2.1	1990	85	####	0.010	1.987 ± 0.105	0.1876 ± 0.0002	2721 ± 2	97
3.1	72	55	####	0.090	1.869 ± 0.093	0.2083 ± 0.0016	2892 ± 13	96
4.1	153	145	####	0.017	1.768 ± 0.076	0.2215 ± 0.0010	2992 ± 7	97
5.1	260	138	####	0.190	2.017 ± 0.136	0.2218 ± 0.0021	2994 ± 15	87
6.1	949	14	####	0.006	1.990 ± 0.095	0.1797 ± 0.0005	2650 ± 5	99
7.1	1529	61	####	0.003	2.025 ± 0.097	0.1852 ± 0.0004	2700 ± 4	96
8.1	1452	41	####	0.004	1.886 ± 0.107	0.1877 ± 0.0011	2722 ± 9	101

all uncertainties in the Table are given at 1 sigma.
Site: x.y, x=grain number, y=analysis number.
Grain and site character: p=prism, eq=small aspect ratio prism, fr=grain fragment
Common Pb correction: comm 206%= percentage of Pb that is non-radiogenic, based on measured 204Pb
and common Pb modelled as Cumming and Richards (1975) for likely age of rock

Table 2. Lu-Hf data for samples.

Sample	$^{174}Hf/^{177}Hf$	1SE	$^{178}Hf/^{177}Hf$	1SE	$^{176}Lu/^{177}Hf$	1SE	Measured $^{176}Hf/^{177}Hf$	1SE	□Hf(0)	±[1]	Initial $^{176}Hf/^{177}Hf$	□Hf(t)	T(DM)2 (Ga)	T(DM) 2 -stage
GGU200892		U/Pb AGE = 3075 ±15 Ma												
200892-1	0.008682	0.000015	1.467413	0.000050	0.000974	0.000009	0.280987	0.000015	-63.6	*0.7*	0.28093	4.6	3.1	3.2
200892-2	0.008659	0.000006	1.467306	0.000023	0.000700	0.000007	0.280913	0.000007	-66.2	*0.5*	0.28087	2.5	3.2	3.3
200892-4	0.008663	0.000015	1.467404	0.000044	0.000900	0.000005	0.280969	0.000016	-64.2	*0.7*	0.28092	4.1	3.2	3.2
200892-5	0.008654	0.000007	1.467506	0.000034	0.000643	0.000005	0.280922	0.000010	-65.9	*0.5*	0.28088	2.9	3.2	3.3
200892-11	0.008678	0.000006	1.467324	0.000021	0.000432	0.000007	0.280909	0.000006	-66.3	*0.5*	0.28088	2.9	3.2	3.3
200892-12	0.008667	0.000006	1.467290	0.000019	0.000621	0.000004	0.280897	0.000007	-66.8	*0.5*	0.28086	2.1	3.2	3.3
200892-13	0.008662	0.000010	1.467370	0.000028	0.000739	0.000003	0.280929	0.000010	-65.6	*0.5*	0.28089	3.0	3.2	3.3
200892-17	0.008660	0.000008	1.467327	0.000023	0.000643	0.000010	0.280918	0.000007	-66.0	*0.5*	0.28088	2.8	3.2	3.3
200892-18	0.008663	0.000006	1.467336	0.000021	0.000520	0.000003	0.280910	0.000007	-66.3	*0.5*	0.28088	2.8	3.2	3.3
200892-20	0.008653	0.000005	1.467356	0.000026	0.000542	0.000010	0.280915	0.000008	-66.1	*0.5*	0.28088	2.9	3.2	3.3
200892-21	0.008660	0.000005	1.467302	0.000034	0.000440	0.000006	0.280887	0.000008	-67.1	*0.5*	0.28086	2.1	3.2	3.3
200892-22	0.008652	0.000006	1.467363	0.000027	0.000449	0.000004	0.280890	0.000008	-67.0	*0.5*	0.28086	2.2	3.2	3.3
Average± 1S.D.					*0.00063*		*0.28092*	*0.00003*	*-65.9*	*1.1*	*0.28088*	*2.9*	*3.2*	*3.3*
GGU200049		U/Pb AGE = 2961±11 Ma												
200499-1	0.008671	0.000007	1.467324	0.000020	0.000432	0.000010	0.280706	0.000007	-73.5	*0.5*	0.28068	-6.9	3.5	3.7
200499-2	0.008650	0.000009	1.467312	0.000022	0.000713	0.000020	0.280720	0.000008	-73.0	*0.5*	0.28068	-7.0	3.5	3.7
200499-3	0.008663	0.000007	1.467391	0.000032	0.000688	0.000002	0.280754	0.000011	-71.8	*0.6*	0.28072	-5.7	3.4	3.6
200499-5	0.008673	0.000007	1.467345	0.000031	0.000473	0.000005	0.280686	0.000008	-74.2	*0.5*	0.28066	-7.7	3.5	3.7
200499-6	0.008658	0.000009	1.467301	0.000025	0.000500	0.000012	0.280677	0.000009	-74.5	*0.5*	0.28065	-8.1	3.5	3.7
200499-7	0.008661	0.000006	1.467312	0.000039	0.000320	0.000003	0.280704	0.000014	-73.6	*0.6*	0.28069	-6.8	3.5	3.7
200499-8	0.008655	0.000007	1.467335	0.000023	0.000545	0.000012	0.280691	0.000007	-74.1	*0.5*	0.28066	-7.7	3.5	3.7
200499-9	0.008664	0.000009	1.467295	0.000025	0.000744	0.000002	0.280756	0.000009	-71.8	*0.5*	0.28071	-5.8	3.4	3.6
200499-11	0.008654	0.000007	1.467274	0.000026	0.000461	0.000010	0.280698	0.000007	-73.8	*0.5*	0.28067	-7.3	3.5	3.7
200499-A	0.008657	0.000007	1.467389	0.000026	0.000903	0.000007	0.280773	0.000007	-71.1	*0.5*	0.28072	-5.5	3.4	3.6
200499-B	0.008657	0.000008	1.467293	0.000024	0.000664	0.000027	0.280724	0.000011	-72.9	*0.6*	0.28069	-6.8	3.5	3.7
200499-C	0.008656	0.000009	1.467341	0.000023	0.000848	0.000017	0.280721	0.000006	-73.0	*0.5*	0.28067	-7.2	3.5	3.7
200499-D	0.008661	0.000014	1.467320	0.000029	0.001230	0.000012	0.280782	0.000010	-70.8	*0.5*	0.28071	-5.8	3.4	3.6
200499-F	0.008656	0.000009	1.467375	0.000028	0.000671	0.000011	0.280743	0.000008	-72.2	*0.5*	0.28070	-6.1	3.5	3.6

Average± 1S.D.					*0.000657*		*0.280724*	*0.000033*	*-72.9*	*0.1*	*0.280687*	*-6.7*	*3.5*	*3.6*
G91/83		U/Pb AGE = 2972 ±12 Ma Ma												
G91/83-1	0.008687	0.000012	1.467744	0.000047	0.000331	0.000011	0.280646	0.000015	-75.6	*0.7*	0.28063	-8.6	3.5	3.8
G91/8-6	0.008673	0.000013	1.467769	0.000059	0.000510	0.000018	0.280729	0.000016	-72.7	*0.8*	0.28070	-6.0	3.5	3.6
G91/83-7	0.008680	0.000011	1.467679	0.000057	0.000526	0.000006	0.280580	0.000015	-78.0	*0.7*	0.28055	-11.4	3.7	3.9
G91/83-12	0.008642	0.000011	1.467900	0.000058	0.000545	0.000023	0.280728	0.000016	-72.7	*0.8*	0.28070	-6.1	3.5	3.6
G91/83-20	0.008640	0.000016	1.467923	0.000055	0.000729	0.000006	0.280737	0.000019	-72.4	*0.8*	0.28070	-6.2	3.5	3.6
G91/83-21	0.008636	0.000015	1.467612	0.000095	0.000787	0.000011	0.280490	0.000032	-81.2	*1.2*	0.28044	-15.1	3.8	4.1
G91/83-22	0.008645	0.000022	1.467771	0.000094	0.001110	0.000034	0.280725	0.000030	-72.9	*1.2*	0.28066	-7.4	3.5	3.7
G91/83-23	0.008658	0.000012	1.467824	0.000053	0.000399	0.000013	0.280787	0.000016	-70.7	*0.8*	0.28076	-3.8	3.4	3.5
G91/83-24	0.008659	0.000011	1.467850	0.000057	0.000291	0.000005	0.280748	0.000015	-72.0	*0.7*	0.28073	-4.9	3.4	3.6
G91/83-25	0.008657	0.000011	1.467645	0.000062	0.000320	0.000013	0.280506	0.000016	-80.6	*0.7*	0.28049	-13.6	3.7	4.0
G91/83-26 c	0.008676	0.000014	1.467703	0.000075	0.000292	0.000022	0.280554	0.000018	-78.9	*0.8*	0.28054	-11.8	3.7	3.9
G91/83-26	0.008667	0.000012	1.467946	0.000090	0.000384	0.000013	0.280756	0.000025	-71.8	*1.0*	0.28073	-4.8	3.4	3.6
G91/83-27	0.008650	0.000014	1.467734	0.000068	0.000791	0.000002	0.280685	0.000018	-74.3	*0.8*	0.28064	-8.2	3.5	3.7
G91/83-29	0.008671	0.000012	1.467797	0.000063	0.000545	0.000006	0.280723	0.000017	-72.9	*0.8*	0.28069	-6.3	3.5	3.6
Average± 1S.D.					*0.000540*		*0.280671*	*0.000006*	*-74.8*	*0.2*	*0.280640*	*-8.2*	*3.5*	*3.7*

CHUR values from Bouvier et al, 2008.

1. This uncertainty is the combined in-run standard error and the external reproducibility of standards for each session added in quadrature.
2. Depleted mantle model ages calculated using 176Hf/177Hf = 0.282785 for the modern upper mantle and 176Lu/177Hf=0.0336.

Two stage model ages are calulated assuming a typical tonalite 176Lu/177Hf=0.009 for the first stage prior to zircon formation.